HU ISSN 1785-6892 in print
HU ISSN 2064-7522 online

DESIGN OF MACHINES AND STRUCTURES

A Publication of the University of Miskolc

Volume 5, Number 2 (2015)

Miskolc University Press
2015

EDITORIAL BOARD

CONTENTS

Design of Machines and Structures, Vol. 5, No. 2 (2015) pp. 5–12.

MODELLING OF MOTORCYCLES AND THEIR COMPONENTS

PAVEL FLORIAN
University of West Bohemia
Univerzitni 8, 306 14 Pilsen
Czech Republic
pflorian@kks.zcu.cz

Abstract: One of the aims of the paper is to develop a mathematical model of a motorcycle using Lagrange equations; the model is verified thanks to ADAMS. Results of multibody simulations are used as inputs for boundary conditions of frame FEM simulation and following topology optimization which results in modifications of the frame design.

Keywords: *Multibody systems, motorcycle dynamics, FEM, topology optimization*

1. Introduction

Design of a motorcycle frame is a complicated task. The frame has to withstand significant dynamic forces without failure. The most reliable method to acquire necessary data is an experiment. However, in case there is no experimental data multibody modelling is arguably the best way to obtain the needed information. At the point when forces and loads are know they can be applied in FEM simulations. Topology optimization is the last step in the process that helps to find the stiffest structure possible taking into account a constraint of limited volume of material that can be used.

2. Mathematical model

2.1. Nonlinear model of a motorcycle

First step of the solution process is to develop a nonlinear mathematical model of a motorcycle. A planar 5-degre-of-freedom model was proposed with following generalized coordinates: x_2 – frame horizontal translation; y_2 – frame translation; φ_2 – frame pitch angle; y_3 – front assembly vertical translation; y_4 – rear assembly vertical translation. A scheme of the model containing generalized coordinates as well as other parameters is shown in Figure 1.
The generalized coordinates are included in vector q as shown in (1).

$$q = [x_2, y_2, \varphi_2, y_3, y_4]^T \tag{1}$$

Lagrange equations (2) were used to develop equations of motion of the system.

$$\frac{d}{dt}\left(\frac{\partial E_k}{\partial \dot{q}_i}\right) - \frac{\partial E_k}{\partial q_i} + \frac{\partial E_p}{\partial q_i} + \frac{\partial \mathcal{R}}{\partial \dot{q}_i} = Q_i \tag{2}$$

Where E_k, E_p and R represent kinetic energy function, potential energy function and Rayleigh dissipation function of the system. Each one of them is listed as the equations below.

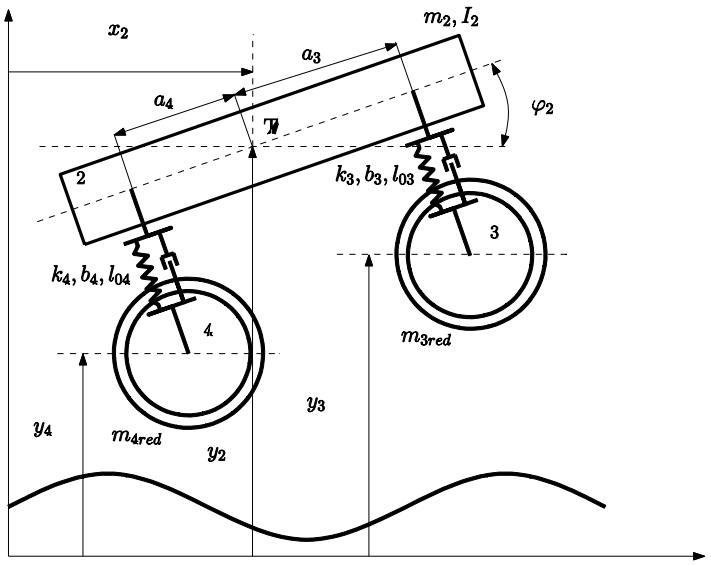

Figure 1. Scheme of the model

$$E_k = \frac{1}{2}\left\{ m\dot{x}_2^2 + I\dot{\varphi}_2^2 + m\dot{y}_2^2 + m_{3red}\left[\frac{d}{dt}\left(\frac{y_2 + a_3\sin\varphi_2 - y_3}{\cos\varphi_2}\right)\right]^2 + m_{4red}\left[\frac{d}{dt}\left(\frac{y_2 - a_4\sin\varphi_2 - y_4}{\cos\varphi_2}\right)\right]^2 \right\} \tag{3}$$

$$E_k = \frac{1}{2}\left[k_3\left(l_{03} - \frac{y_2 + a_3\sin\varphi_2 - y_3}{\cos\varphi_2}\right)^2 + k_4\left(l_{04} - \frac{y_2 - a_3\sin\varphi_{2-} y_4}{\cos\varphi_2}\right)^2 \right] \tag{4}$$

$$\mathcal{R} = \frac{1}{2}\left\{ b_3\left[\frac{d}{dt}\left(\frac{y_2 + a_3\sin\varphi_2 - y_3}{\cos\varphi_2}\right)\right]^2 + b_4\left[\frac{d}{dt}\left(\frac{y_2 - a_3\sin\varphi_2 - y_4}{\cos\varphi_2}\right)\right]^2 \right\} \tag{5}$$

After conducting partial derivatives according to (2) a mass matrix M, a stiffness matrix K and a damping matrix B can be developed as shown below.

$$\boldsymbol{M} = \begin{bmatrix} m & 0 & 0 & 0 & 0 \\ 0 & m & 0 & 0 & 0 \\ 0 & 0 & I & 0 & 0 \\ 0 & 0 & 0 & m_{3red} & 0 \\ 0 & 0 & 0 & 0 & m_{4red} \end{bmatrix} \tag{6}$$

$$\boldsymbol{K} = \begin{bmatrix} 0 & 0 & 0 & 0 & 0 \\ 0 & k_3 + k_4 & \dfrac{(k_3 a_3 - k_4 a_4)\sin\varphi_2}{\varphi_2} & -k_3 & -k_4 \\ 0 & (k_3 a_3 - k_4 a_4)\cos\varphi_2 & \dfrac{(k_3 {a_3}^2 - k_4 {a_4}^2)\sin 2\varphi_2}{2\varphi_2} & -k_3 a_3 \cos\varphi_2 & -k_4 a_4 \cos\varphi_2 \\ 0 & -k_3 & \dfrac{-k_3 a_3 \sin\varphi_2}{\varphi_2} & k_3 & 0 \\ 0 & -k_4 & \dfrac{k_4 a_4 \sin\varphi_2}{\varphi_2} & 0 & k_4 \end{bmatrix} \tag{7}$$

$$\boldsymbol{B} = \begin{bmatrix} 0 & 0 & 0 & 0 & 0 \\ 0 & b_3 + b_4 & (b_3 a_3 - b_4 a_4)\cos\varphi_2 & -b_3 & -b_4 \\ 0 & (b_3 a_3 - b_4 a_4)\cos\varphi_2 & (b_3 {a_3}^2 - b {a_4}^2)\cos^2\varphi_2 & b_3 a_3 \cos\varphi_2 & b_4 a_4 \cos\varphi_2 \\ 0 & -b_3 & -b_3 a_3 \cos\varphi_2 & b_3 & 0 \\ 0 & -b_4 & b_4 a_4 \sin\varphi_2 & 0 & b_4 \end{bmatrix} \tag{8}$$

The stiffness matrix and the damping matrix are both not constant and depend on the generalized coordinate φ_2 which means the system is nonlinear and provides more accurate results as displacements increase. However, this also places requirements on the integration method of the motion equations itself.

2.2. Tyre contact model

Interaction between tyres and road is a significant source of forces that act on the frame. In this case longitudinal driving and braking forces are neglected and the key task is to obtain normal contact forces. As stated previously the whole model is planar therefore lateral cornering forces are not taken into account either. The model of the tyre contact is shown in Figure 2.

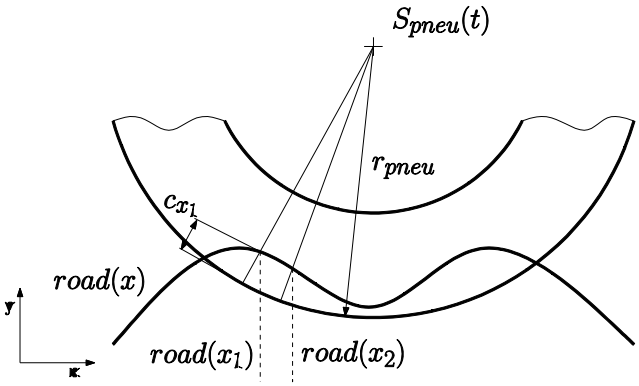

Figure 2. Tyre contact model

Let's assume that the location of tyre centre in known at any time. In case that any point of road surface is closer to the tyre centre than tyre radius a contact pressure exerting on the tyre can be calculated as

$$p_k = k_p c \tag{9}$$

Where $k_p[N/m^2]$ describes stiffness characteristics of the tyre and c is the difference between the tyre radius and the distance. Differential normal force can be obtained according to (10).

$$dN = k_p c ds \tag{10}$$

Differential ds relates to tyre arc. Differential normal force is always perpendicular to the road surface. For our problem it is crucial to determine its components in horizontal and vertical direction. This can be accomplished by using derivative of road function as described in the following equations.

$$dN_x = k_p c \sin\left(\arctan\frac{droad}{dx}\right) dx \tag{11}$$

$$dN_y = k_p c \cos\left(\arctan\frac{droad}{dx}\right) dx \tag{12}$$

In order to determine the components of the actual normal force, integration is conducted as the very last step.

$$N_x = \int_{x(S_{pneu})-r_{pneu}}^{x(S_{pneu})+r_{pneu}} dN_x \tag{13}$$

$$N_y = \int_{y(S_{pneu})-r_{pneu}}^{y(S_{pneu})+r_{pneu}} dN_x \tag{14}$$

The tyre contact model proposed above is based on elastic contact model. Tyre hysteresis effects can be taken into consideration as well assuming damping forces have similar character to normal contact forces as stated in the following equation.

$$N_b = \dot{c} N \frac{b_k}{k_k} \tag{15}$$

The variable $\dot{c}$ from previous equation relates to tyre deformation rate.

3. Numerical integration of the equations of motion

Once we acquired the forces acting on tyres we can proceed to solution process of the motion equations with MATLAB. Set of 5 nonlinear ordinary differential equations is summed up in the (16).

$$\boldsymbol{M}\ddot{\boldsymbol{q}}_{(t)} + \boldsymbol{B}\dot{\boldsymbol{q}}_{(t)} + \boldsymbol{K}\boldsymbol{q}_{(t)} = \boldsymbol{f}_{n(\dot{\boldsymbol{q}},\boldsymbol{q},t)} \tag{16}$$

Constant average acceleration integration method was used due to its relative simplicity and numerical stability. This method is predictor-corrector based as the system in question is nonlinear. A road function was designed using modified sin functions to represent an obstacle, which is supposed to cause a loss of contact between the tyres and the road. In this way a jump of a motorcycle can be simulated.

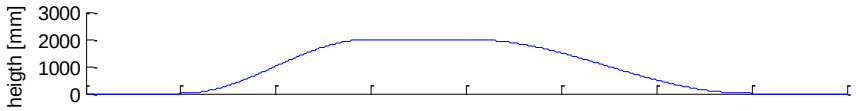

Figure 3. Road profile

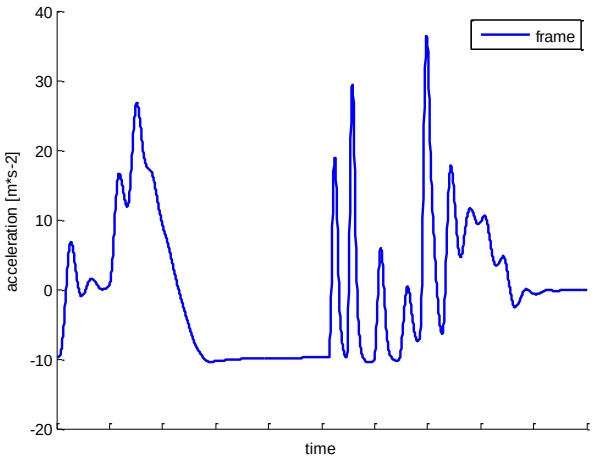

Figure 4. Frame acceleration results

Acceleration results are shown in the figures below. In Figure 4 there are acceleration results of the frame. The initial steep increase relates to the beginning of the obstacle. As the acceleration drops to approximately -10 $\mathbf{ms^{-2}}$ it means that the tyres lost contact with surface. The peak values occur after landing reaching 36 $\mathbf{ms^{-2}}$. Acceleration results of front and rear assembly in Figure 5 can be explained in a similar way.

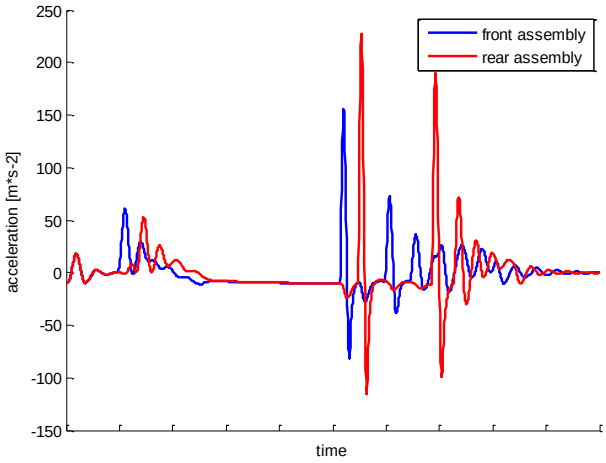

Figure 5. Front and rear assembly acceleration results

4. Model verification

The mathematical model that was developed provides reasonable results; however, further verification is necessary. In order to do so, ADAMS/VI-Motorcycle module was used to compare results. In Figure 6 there is a motorcycle model in VI-Motorcycle interface running over an obstacle defined in the same as in the MATLAB model.

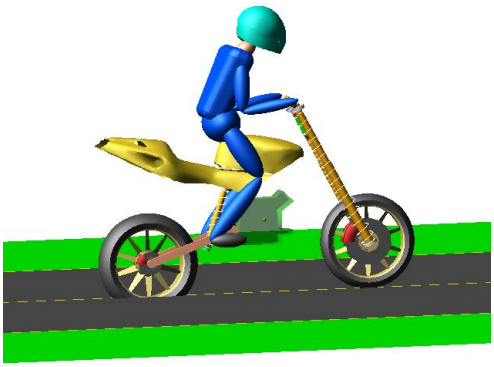

Figure 6. VI-Motorcycle model

In Figure 7 there are acceleration results of front assembly in ADAMS and MATLAB. In this simulation tyre damping properties were neglected in MATLAB, which explains the key difference between both curves.

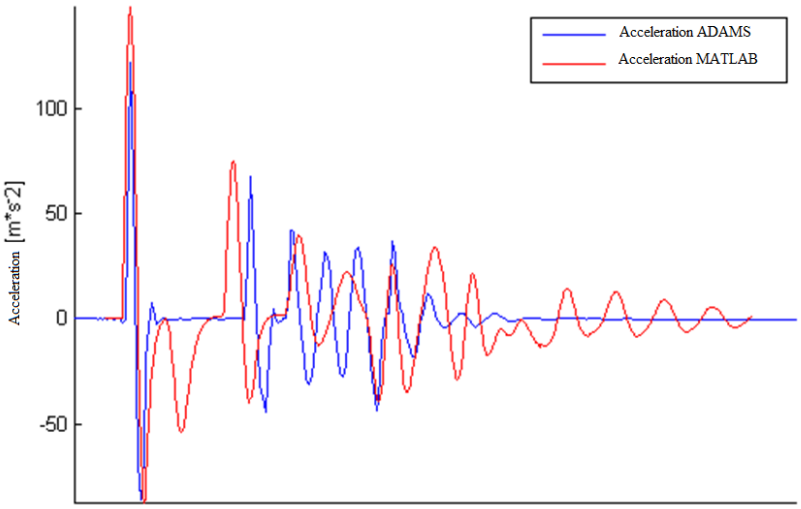

Figure 7. Front assembly acceleration results

5. FEM Simulation

The last step that concludes this paper is a FEM simulation followed by a topology optimization. Boundary conditions that are necessary for the simulation were obtained in the previous step. As it can be seen in Figure 8 the frame is an open tubular frame, which means an engine plays major role in overall stiffness. Engine stiffness properties were determined separately and these effects were expressed by 1D CBUSH elements in the whole model. Topology optimization enabled design modifications resulting in stiffness increase by 33% while saving 200g in weight. Lower overall values of stress were also achieved thanks to topology optimization.

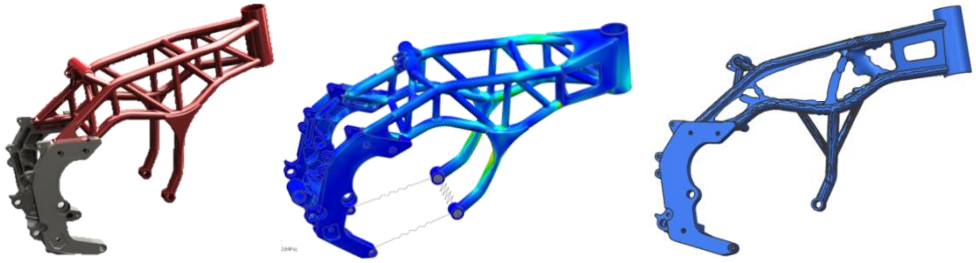

Figure 8. CAD, FEM and Topology optimization model

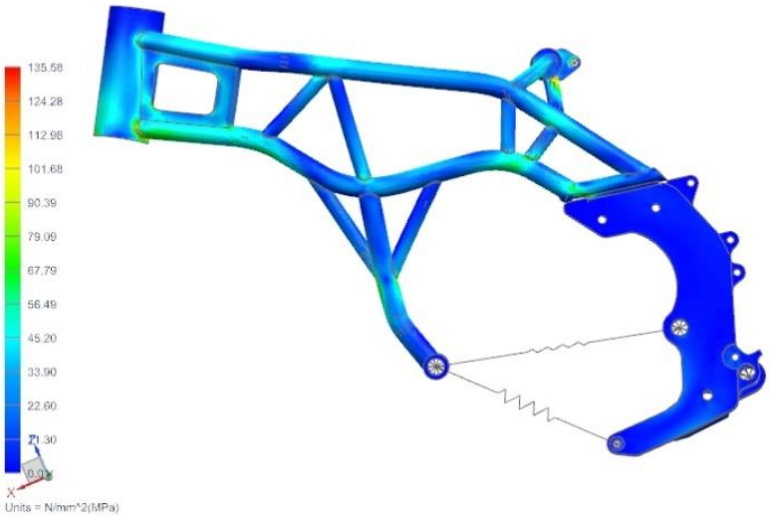

Figure 9. FEM results after topology optimization

6. Summary

Design of a racing motorcycle frame is a complicated task. Without previous experience is experimental data multibody modelling is arguably the only way to obtain boundary conditions for FEM simulations. Nevertheless, to describe motorcycle behaviour and exerting forces properly a large number of simulations would be necessary. Therefore the data acquired in this paper are more suited to compare design alternatives instead of exact FE modelling. Topology optimization is a powerful tool allowing shortening the whole design process in order to find optimal solution.

7. References

[1] DUPAL, J.: *Výpočtové metody mechaniky.* Učební text. ZČU FAV, 2004.
[2] COSSALTER, V.: *Motorcycle Dynamics.* Lulu Press, London, 2006.
[3] FOALE, T.: *Motorcycle Handling and Chassis Design, the art and science.* Spain, 2002.

Design of Machines and Structures, Vol. 5, No. 2 (2015) pp. 13–16.

DESIGNING PRAM TESTING EQUIPMENT

DÁNIEL HERBST–ÁGNES TAKÁCS
University of Miskolc, H-3515 Miskolc-Egyetemváros, Hungary
takacs.agnes@uni-miskolc.hu

Abstract: The birth of a child is the biggest completion in one's life as due to the biological functions one can forward their genetic values by conception, later morality in education. Human life is a great value, thus we can say the vehicle carrying the baby or toddler should be safe and reliable. The article shows the consideration of equipment that is suitable for testing the adult handle.

Keywords: *pram, load test, designing considerations, environmental awareness*

1. The operative standard and the chosen test

The perfect operation of a child pram is guaranteed by testing in line with the appropriate standard of MSZ EN 1888-2012. The durability test against the lifting-pressing stress of the handguard of the adult's handhold has been chosen out of a great number of tests.

The standard defines an optimal pram construction with appropriate size and reinforcement points, as well as the test weights put in the pram. For a pram shorter than 800mm two different test weights can be used, one of them is "test weight A", which is (9+0.01/0) kg, the other is "test weight B", which weighs (15+0.01/0) kg. For prams longer than 800 mm "test weight F" is applied, which weighs (13+0.01/0) kg.

The handhold can be pressed with the maximum strength up to 450N, this way pressing the rear structural elements of the pram as far as the front wheels are considered up to the front wheels' 120±10mm. Lifting the load of the pressed structure means lifting the rear wheels onto the height of 120±10mm. The cycle shown in the first passage should be repeated 3000 times, with (15±2) cycle number per minute.

This phase of the test is to study durability while crossing a hardshoulder. The second phase can be described by a more simple cycle during which by raising the handhold and lifting the rear wheels the structure moves up until they reach the height of 120±10mm. Full pressure moves onto the first wheels of the pram. After that comes letting the wheels down, in a more careful way, that is making the pram slower.

The second phase of the test has 7000 cycles, the cycle number per minute has been the same as it was in the first task (15±2). All in all, the test studies the durability of the pram through the adult handholder. A pram passes the test only if it survives 10,000 cycles without any serious damage.

2. Summary of designing

The first step after the patent and segmented market research was followed by the conceptualised designing process, in which different forms of solutions appeared from the abstract function analysis to exact function structures. Studying the different versions of solutions according to the system of showing positive values with Copeland value analysing method, the optimal version appeared which gave guidelines for the later designing process. Important security and material usage restrictions and requirements were considered, which could influence the forming of construction, paying attention to the importance of the environmentally friendly design of the equipment, and safe usage.

For the forming of the construction we needed to make clear the force requirement of moving the pram at given parametres.

During the study this force means a periodical load on the elements of the testing equipment, this way we need sizing for fatigue, which can be done by the Soderberg procedure. First, the procedure for the general case was described, which later was used for the parts of the clamp device.

With the help of sizing procedure the clamp device was optimised with a finite element software.

3. Design considerations

Considerations refer to several fields, for example, the regulation of 16/2008 (VIII. 30.) NFGM, which is a regulation for the safety requirements and maintenance of machines.

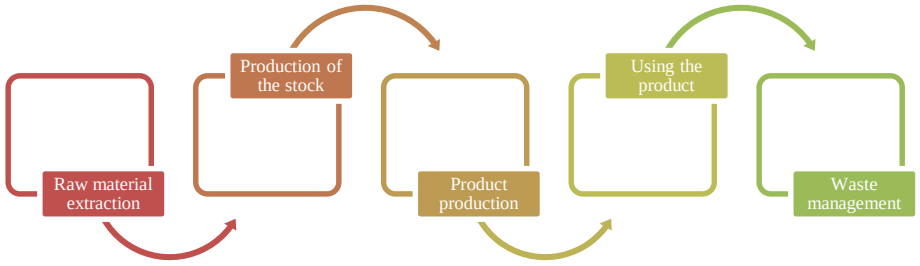

Figure 1. Life-cycle of a product-material [2]

It is important to approach designing from environmentally friendly perspec-tives as environment resources are limited and their usage takes place in an irresponsible way. In the present case circumstances coming from the life cycles of the equipment dominate.

Raw materials should be easily accessible from trade, this way energy resources are minimized as raw materials are produced in bulk, or the tool part is made more efficiently than it could be at home.

We have to use parts that make the structure more simple (e.g. function contraction), this way the required number of elements could be decreased.

The raw material parts also should be produced with minimal environment load, or at least the recycling of the raw materials should be easy.

The elements used in the device should be replaceable, or at least recyclable. This way we can increase the lifespan of the device and the raw material, so there less material will be needed to extract.

At assembly or at uniting certain parts into bigger units dissociable technologies should be used technologies taking into consideration the possibility that it can be used for other tests, as well as for possible replacement of tools.

Special tools that have to be manufactured should not be needed for the assembly of the equipment. Safety elements should be used, which prevent the failure of parts manufactured with bigger environmental load.

4. Application of considerations

The support structure of the equipment could be made of aluminum profile, with a profile shape from any other market, or general steel in the appropriate form. In the case of aluprofile, fitting elements to each other takes place through nitches and flexible nuts with corner elements and switching element available with profiles.

Uniting a working element and its course of elements moved by it can mean function uniting (like a pneumatic actuator).

The effort for the most simple way of forming the number of parts can be decreasing the number of parts. For example, in the case of an aluprofile the sheet under the pram could be placed on the walls of nitches of the aluprofiles, and it is enough to tie them in the end.

5. Outlook onto the issue of material usage

It can be stated that raw materials are of great importance in any designed equipment or machine. We usually choose the materials according to their mechanical properties that are necessary for the aspect of function completion; however, there are other trends, which lead to smaller environmental load. Certainly we have to pay attention in the case of materials to different effect carriers through which processing procedure we should take over to achieve the appropriate geometry and size. We can find a lot of charts and graphs about the expenditure of certain materials, for example, the chart of energy needs of the Autodesk which was worked out for the economical planning. In the chart the load of certain material groups is compared with the expenditure on energy.
(Figure 2, http://manufacturingtoolbox.typepad.com/my-blog/2012/02/)

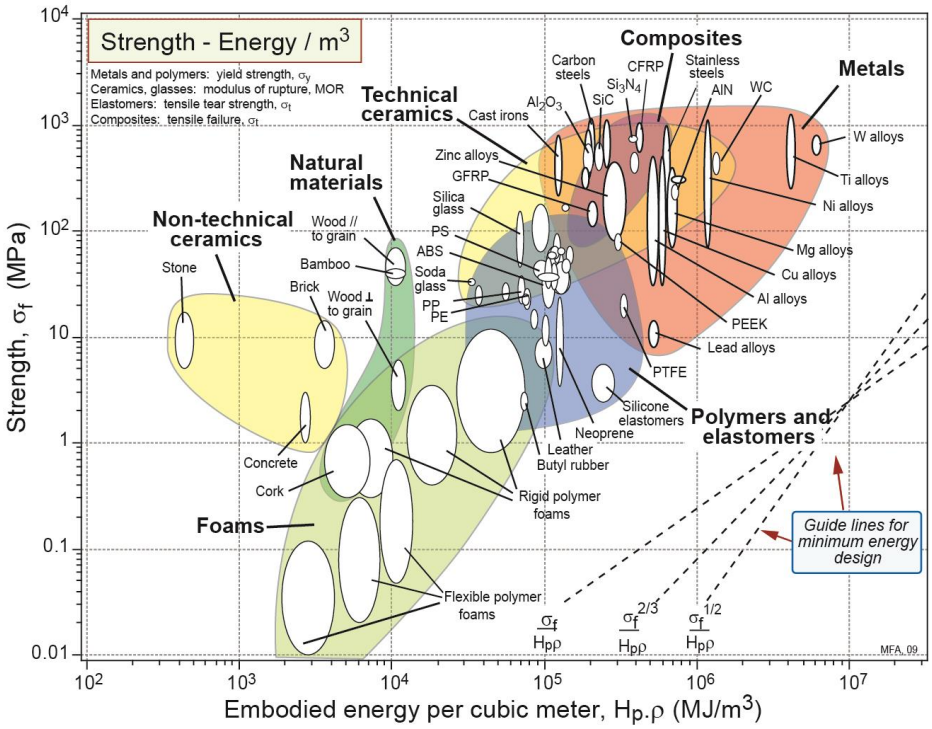

Figure 2. Energy necessity diagram

6. Acknowledgement

This research was supported by the European Union and the State of Hungary, co-financed by the European Social Fund in the framework of TÁMOP-4.2.4.A/2-11/1-2012-0001 'National Excellence Program'.

7. References

[1] LUTTROPP, C.–LAGERSTEDT, J.: EcoDesign and The Ten Golden Rules: generic advice for merging environmental aspects into product development. *Journal of Cleaner Production*, 2006, Elsevier.

[2] OTTO, K.–WOOD, K.: *Product Design – Techniques in Reverse Engineering and New Product Development.* Prentice Hall, 2008.

[3] PAHL, G.–BEITZ, W.: *Engineering Design – A Systematic Approach.* Springer Verlag, London, 2005.

[4] MAZINOVA, I.: Designers and Sustainability. *Design of Machines and Structures*, Vol. 5, Nr. 1, Miskolc University Press, Miskolc, 2015.

Design of Machines and Structures, Vol. 5, No. 2 (2015) pp. 17–29.

BRANCH SHAKER DESIGNING PROJECT

GERGŐ NAGY–BETTINA SPISÁK–ATTILA SZÓJA–ISTVÁN SZÁNTAI–
JARMO JALKANEN–JARNO MATTILA–MARIA RENTOLA–
TIBOR PUSKÁS
University of Miskolc, Department of Machine and Product Design
3515 Miskolc-Egyetemváros
JAMK University of Applied Sciences
PO BOX 207, FI-40101 Jyväskylä, Finland
nagy.gergo@schaeffler.com

Abstract: In this paper a new hand tool designing project will be represented. The background of the project is an international co-operation between JAMK University of Applied Sciences from Finland and University of Miskolc. The main task was created by Robert Bosch Power Tool Ltd. to design a multifunctional battery operated garden hand tool. For the more effective work was organized two mixed group from Hungarian and Finnish students. The competition between the groups simulates the real life, where the companies have to create better product than the others.

Keywords: *hand tool, branch shaker, project planning*

1. Introduction

The first and most important task – like in every project – was defining the roles of the members. It was necessary to find the suitable positions for the members in the project. The most important roles were marketing, quality, purchasing, designing and the engineering side (Figure 1).

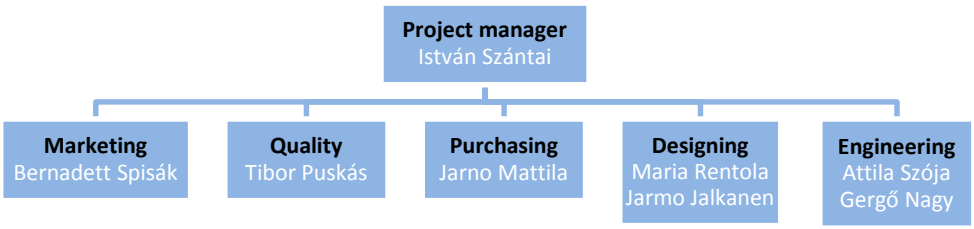

Figure 1. Positions of the members

Project manager was István Szántai, he leaded the team. He was responsible for finishing the project. Every team member got the assignments from him. He supervised everybody's work, organized the meetings and sent the update reports to the supervisors.

Marketing person was Bernadett Spisák. Her most important job was to keep contact with the potential customers and map the competitive products.

Quality man was Tibor Puskás. His task was to oversee that the choosing of the parts were right and economic. He observed that every part of the construction satisfy the requirements of the customers, so he reviewed those ideas that were not right. He made the connection between the engineers and the marketing person.

Purchasing was Jarno Mattila's job. He handled to find the right components, and got information about its cost. On top of that, he created a costing table. From this, he could calculate a competitive price for the product. Purchasing and marketing person worked together to find out the price customers are willing to pay.

Industrial designers and mechanical engineers had two different kinds of tasks, but their jobs were connected. Attila Szója and Gergő Nagy were the mechanical engineers and Maria Rentola, Jarmo Jalkanen were the industrial designers. Engineers designed certain parts of the product, like the motor, battery etc. Industrial designers made the conception of the house for these tool parts, which are ergonomics and comfortable for the customers.

2. First steps of the project – Collecting ideas

In the first step there was the hardest task to figure out a new tool. For this, the project members started brainstorming on what kind of works people can do in the garden. These works are e.g.: grass cutting, branch shaking, leaves collecting, planting, digging, fruit collecting, cleaning garden tables and chairs, root removing and so on.

After that, the group started to think about what kind of tool is not on the market yet. It was known the Bosch products are good at grass cutting and hedge trimming, so the project concentrated on the planting, digging, fruit collecting and root removing work. From these kinds of gardening jobs three possible tools were imagined for future design. These tools are: seed feeder, weed remover and branch shaker.

To find the best tool it was necessary to compare these tools in different aspects like how often used, similar products in the market, weight, size, possible price of the product.

The team thought that people are able to use the branch shaker to shake many different fruits down from the trees and they can use it for leaves shaking as well. The group did not find such branch shaker tool on the market that is operated with battery, as well as this shaker technique is used in more tools and machines for harvesting, so in this tool could work also. The branch shaker had so many advantages as it was chosen to design.

3. Designing the tool

3.1. Designing the shaker head

Searching for patents of different head types is very important task, because stealing anybody's idea is not correct. However, the searching is useful, because we can use the old, forgotten ideas to design a new machine.

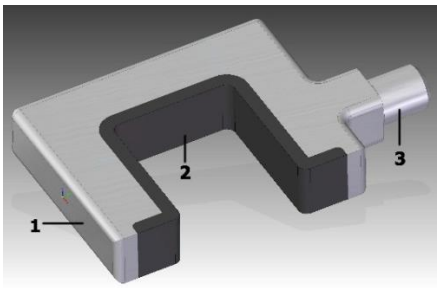

Figure 2. Fixed head (first 3D model)

Many conceptions were created during design. For example: fixed-, adjustable-, handle operated-, automatic head. All of these were analysed, and the most suitable was chosen.

The chosen head has fixed size (Figure 2). This is not adjustable. People can grab branches under the size of the head's mouth. If the internal size of the mouth is 40 mm, than man can grab a branch that has a diameter of 40 mm, or smaller. Some measurements were made to define the average branch diameter and shaker force than the conclusions were described. The internal size of the mouth can be maximum 60 mm. Larger mouth is unnecessary. The head part 1 material is a strong steel or aluminium alloy. Part 2 is a flexible deposit. Its material is rubber. This head can be one part with the rod, or it can be connectable to the rod in point, part 3.

Different working situations were examined and the fixed head was chosen. People can grab the branch with this type of head and it works on other tools too. Its design is easier than the others.

3.2. Finite element analysis of the head

It is an important exercise because it could simulate the working situation and the group can optimize the critical parts. We made the analysis more times. Two materials were chosen, an aluminium alloy and ABS plastic material. The results of the analysis were compared with the material properties. The most important things were the deformation, and the equivalent stress in the material of the head. The analysis was made in Ansys 14 and Solid works.

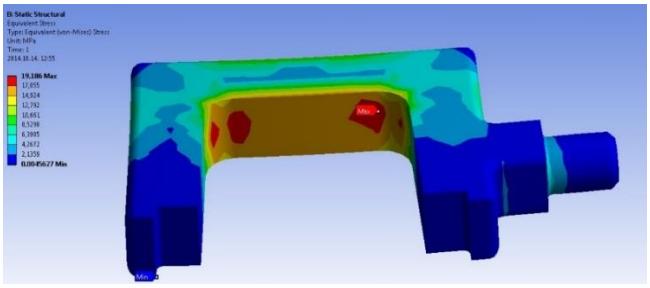

Figure 3. Finite element analysis of the head

Plastic material is cheaper and lighter than aluminium, but its strength would not be enough, just with larger size, that is why the material of the head has to be aluminium alloy.

Results of the analysis showed, the form of the head is not the optimal. It was necessary to make an optimization. The highest stress values were in the inner corner of the mouth. It was necessary to apply bigger radius in this corner. So the loading distributes evenly in the head. The other reason was the nicer form. It looks prettier with the modified shape (Figure 4).

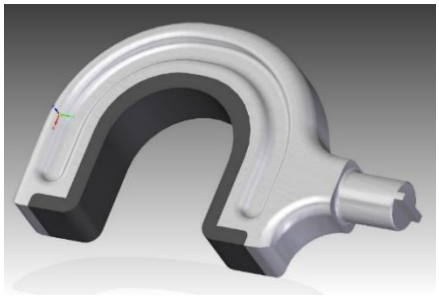

Figure 4. New design of the head

3.3. Connection between the head and the arm of the transmission

This tool is multifunctional. First function is branch shaking; second one is branch cutting. It is necessary to change the head and the saw on this machine. Our group had to create an adapter to the arm of the transmission. This adapter is able to fix the head or the jigsaw fixer adapter.

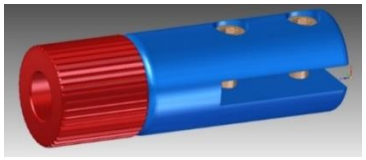

Figure 5. Adapter for fixing the head and jigsaw adapter

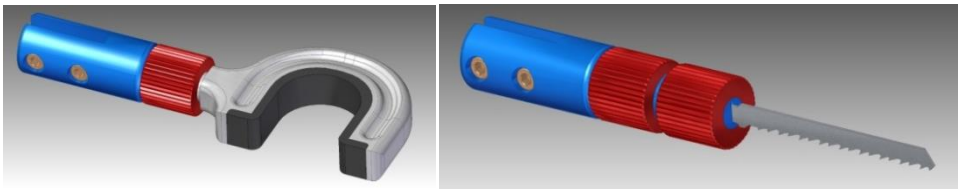

Figure 6. Shaker head and jigsaw blade with the adapter

3.4. Rod connection

Our group found some patents for rod connection. There were connectable and telescopic too. Drusiani Franco had a great idea. He invented the telescopic rod connection for agricultural tools on the 20th June 1995. It is lapsed, so we could use it up free.

A similar solution was applied in case of the branch shaker. This connection type operates as follows. There is an outer tube and there is a threaded connection element fixed in this tube. There is an inner tube with closing element. There is a tapered clamping element next to the threaded element. There is a grip on these parts with an internally threaded element. If we turn the grip in one direction, we can release the clamping, so we can pull the inner tube to full length. If we turn the grip reverse, we can make the clamping, so the inner tube is fixed in that position (Figure 7).

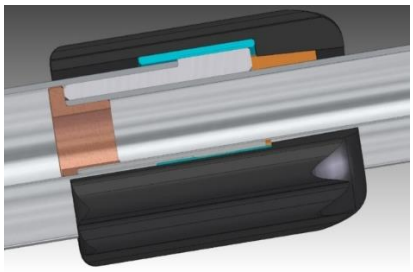

Figure 7. Rod connection in case of branch shaker

Finite element analysis is also important in case of the rod. It was necessary to run dynamic analysis because shaking and cutting load change in time.

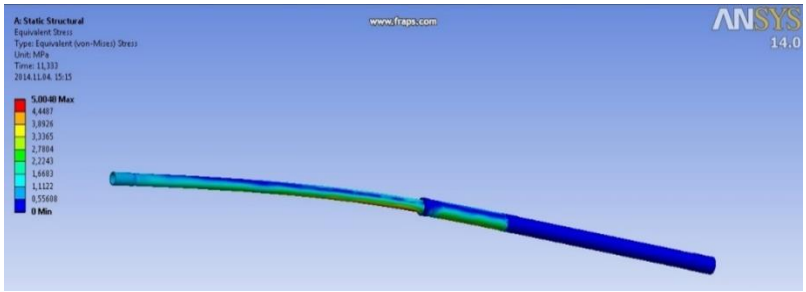

Figure 8. Finite element analysis of the rod

There are two fixed support on the rod, because the customer grabs the tool with two hands. The position of the electrical hand tool during the work is not horizontal, but 45° angle to the ground. There is not only one load, but there are two. These loads change in time. One of them is the weight of the motor and the head; it is about 20 N. This load is at the end of the rod and it points towards the ground. The other load is the shaker force. It is in direction of the rod. The shaker force is about 200 N,

but it is not the maximal. We have to make analysis with overload. Overload is 500 N. It simulates if the customer grabs the branch with this tool and pulls it. The standard earth gravity also takes its effect.

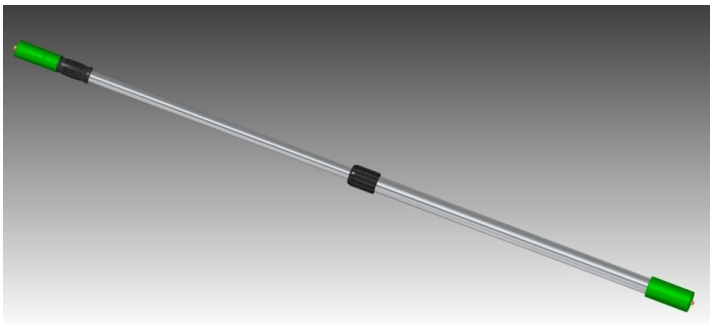

Figure 9. Full length of the rod with shock absorbers

Figure 9 shows the rod design. The weight of the rod without the shock absorbers is 2,77 kg.

3.5. Shock Absorber Unit

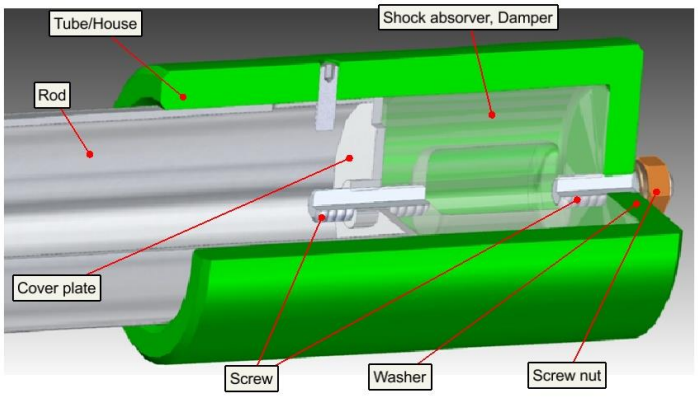

Figure 10. Shock-absorber unit

It was necessary to create a unit that reduces vibration of the branch shaking. It is obvious, that vibration is harmful for human's body, so vibration absorbing was an important part of engineering design. Inside and outside diameters were important, because the vibration absorber involved the bottom of the rod. Therefore, there is housing for the tube. This house is cylindrical. Since it is necessary to support the rod, the house has 75 mm support hole. In the house there is an extra place for the shock absorber. The damper is under the rod. Shock absorber consists of three main parts. One of them is the silicon cylinder that is responsible for absorbing. This is

due to the fact, that silicon has big capability for shape deformation. Other two parts are screws, one for the rod and one for the house fixing. Shock reducing process is simple. When the motor starts and the shaker is working, there is high vibration in the entire rod. Therefore, vibration causes deformation in the silicon part of damper. Silicon is hollow, so there is enough space for deformation (Figure 10).

3.6. Motor choosing and movement conversion

The main part of the tool is the motor. This part is responsible for how hard the tool can push and pull the branch and how much time the tool works. A quick alternate movement was needed to the branch shaker that is why a movement converter part had to take place into the tool that changes the motor rotation to alternate moving. The easiest way for this transmission was a couple of gear and an arm part, where the bigger gear is an eccentric gear (Figure 11).

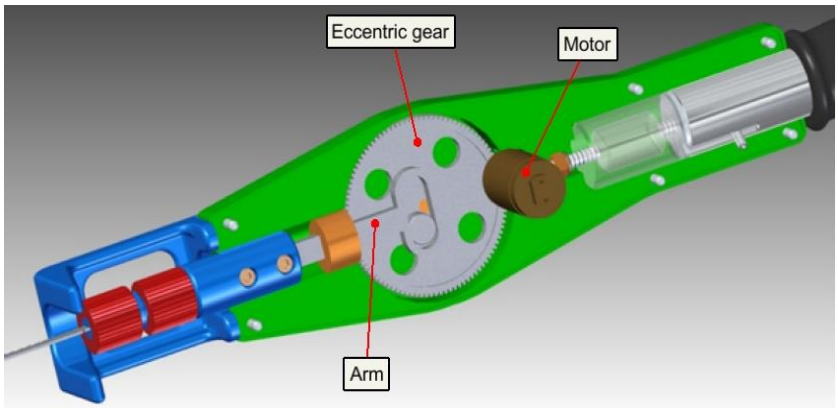

Figure 11. Motor and gears for alternate moving

It was necessary to determine how large force is needed for the shaking and how long the customers would like to use the tool in one time. Based on marketing surveys users do not plan to work with the tool above one an hour at once. Measurement showed that a 50 N force is enough to move thinner branch.

Estimating the working time of the tool was created in SciLab program, where more factors were needed to define previously.

It was very important to define the mass moving by the motor. The mass of the rod would weight too much for the motor to move that is why the motor house is at the top of the rod, so in this case the motor has to move just the mass of the head and arm parts.

Other essential elements of the tool were the transmission of the gears and the eccentricity. These numbers were taken from a Bosch hedge trimmer's parameters.

The third factor was the motor that was chosen for big stall torque, big no load speed and a suitable battery capacity.

The program tested the designed tool according to these chosen parameters and we found that the tool can work between 20–30 minutes if the shaking force is between 50–80 N. Consequently if we have two battery packs we could reach the 60 minutes working time with the tool.

4. FMEA – Failure mode and effect analysing

Risk analysis tools are used to identify possible risks of the process or a target. It shows in what way the product does not fulfil customers' requirements and what are the effects of the risk to the customer. Design FMEA is a great tool to help designing and quality personnel to detect the highest risks of the new product before the process has gone too far. This way it is easier to take note of the biggest issues when you are designing the product and you do not have to make big critical changes later. It is important to find out all the risks that are harmful or dangerous to the final user of the product. During engineering design of the product you must pay attention to all of these risks and figure out the best solutions to prevent these harmful things to come true in the final product.

At the beginning of this project-FMEA our group started to list all different kind of risks from as many different aspects as possible. Group wanted to find risks that especially concerns about user safety and satisfaction of using the product. Listed risks were collected to an Excel template. After this the risks were valuated from 1÷10 according to three different factors: severity (SEV), occurrence (OCC) and detection (DET). After valuing the risks these three factors were multiplied together to get the Risk Priority Number (RPN=1÷1000). Group wanted to keep the RPN below 100 to ensure that the risk is low enough because most of the risks concerned about user safety.

Highest risks that were found and needed actions were the shaking of the tool, weight of the tool, protection against water and accidental starting of the product. Shaking can be reduced by anti-vibration solutions in handles and rod connections. For the weight of the tool it is important to use light materials. Water proofing is necessary for this tool because it is used outside and it can get in touch with water. Accidental starting of the product can be minimized with two-button start.

5. Purchasing

There was one main task for purchasing. Calculate the final product price with materials choosing, which satisfy the quality requirements. Besides it was decided that gross margin profit has to be over 40%.

Calculating material costs was a little hard because distributors do not always show prices for materials in websites. After investigation, it was the best way to use Alibaba.com for searching the materials and prices. At this point we could only use material costs because we did not know the shipping costs. Because of that prices, which are used in calculation, are a bit higher than in distributor sites. Excel table is used for material cost calculation and weight of the product calculation also. A part of this table can be seen in Table 1.

Table 1
Purchasing chart

Part	**Quantity**	**Price/piece (€)**	**Total price (€)**	**Mass (kg)**
Battery cell	2*10	1,25	25	0,38
Battery housing	1	0,5	0,5	0,08
Lower house	1	1,2	1,2	0,3
Lower rod	1	4	4	1
Upper rod	1	4	4	0,82
Motor	1	1,65	1,65	0,34
….	….	….	….	….
Total material cost per product:	59,11 €		total mass:	6 kg

5.1. Labour cost

Labour cost per product is needed to know also for the total manufacturing price. Formula is: $x = (w * p)/(d * s)$, where x is labor cost per product, w is monthly wage, p is people per shift, d is working days per month and s is products per shift. Values which were used:

- 500 € monthly wage
- 7 people per shift
- 21,7 working days per month
- 1000 products per shift

With these values labour cost per product is only 0,16 €.

5.2. Market price

Formula for gross margin profit is $g = (t - m)/t$, where g is gross margin profit, m is manufacturing price and t is total market price. Converting this formula to this form $t = m/(1 - g)$. For manufacturing price sum from labor cost and material cost are used and it is 59.27€. Gross margin profit is 40%. With these values market price is 98.79€. Because it is much lower price than competitive products, 125 € is the final market price for our product.

6. Marketing

6.1. Similar products

At the beginning of the project, marketing job was to find similar products. It was necessary because this way we were able to collect ideas for our tool. On the internet, there were some items, which had the same function to shake the branches. They were compared in different aspects. Three out of five works with fuel, which makes the tool expensive, but the effectiveness of them is very good. They are heavy so the using of them is hard for elderly people. The other two items work with battery and electricity. At the end of the rod there is a rake which is moveable. These ones are

used only for olive shaking. They are light so they can be used easily. We tried to combine these tools.

6.2. Survey

Another important job of the marketing person was to keep contact with the potential customers. So she made a survey. Making a questionnaire is a basic task of a product design, as we can measure the future customers' needs. With a questionnaire, we are able to collect large number of anonymous reviews. It is easily processed, and we can make statistical analysis of the data. However, we have to pay attention, because if the question is not properly provided, then a problem may arise later.

6.3. Making the survey

We had to make a short, essential survey. Many questions were collected, which should be asked from the customers. The most important questions were chosen. That is how we got the following ones:

1. What is your gender?
2. What is your age?
3. Which is your country?
4. Do you have fruit trees or bushes at home?
5. What kind of fruit tree/ trees do you have?
6. How do you harvest your fruit tree?
7. Would you use a tool that helps you shake the fruits down?
8. If you have a fruit shaker tool with cutting head would you use it for branch cutting?
9. Would you use this branch shaker tool to shake the leaves down?
10. How much time would you use this branch shaker tool for one occasion?
11. How much would you pay for a tree shaker?
12. How important would be for you the weight of the tool?
13. How important would be for you the shape of the tool?
14. How important would be for you the size of place taking of the tool?

There are two different kinds of question. It can be seen that the first three questions are ordinary ones. It is important to know, who is the answerer, because with this it can be predicted, who are the future users. There were specific questions too; here we asked important things about our tool. They were needed because this way we could conclude, which are the most relevant things of our tool. It was necessary to know what kind of trees the future users have, because this way we could estimate how much force is needed to move a branch of the given tree. Our job was to make a multifunction tool. Our idea was to use it for branch cutting beside the branch shaking. From all of these the most important is, if the customer will use this tool. Another one is how much the users would pay for it.

6.4. Some results of the survey on diagram

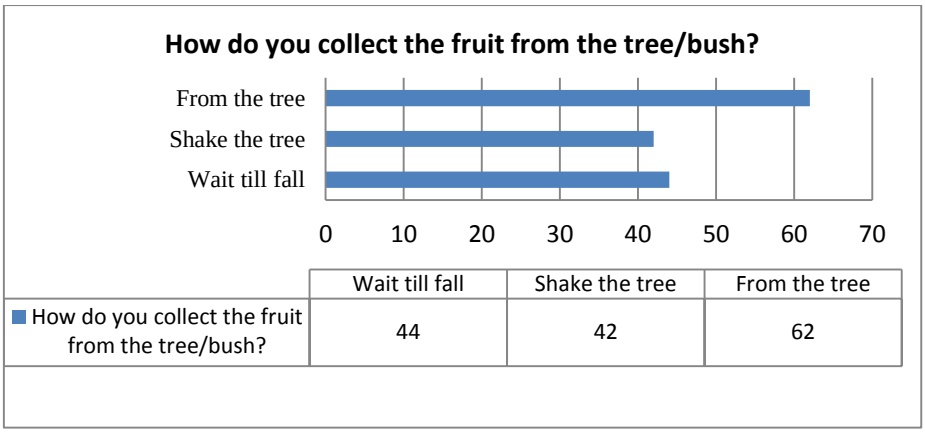

Figure 12. Fruit collecting method

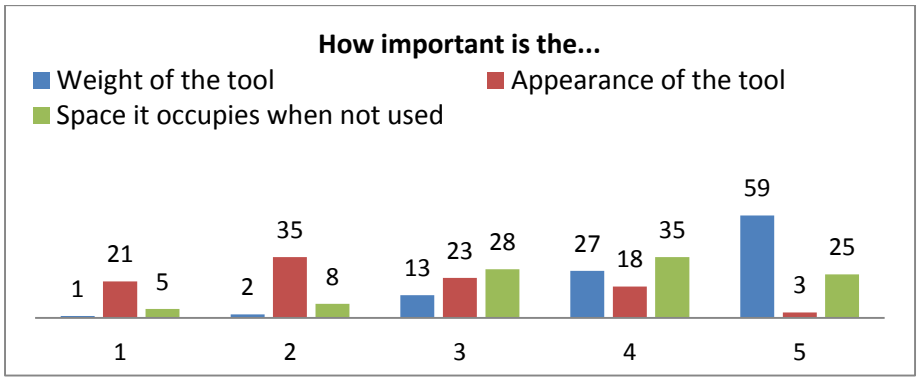

Figure 13. Importance of aspects (1 – not important, 5 – important,)

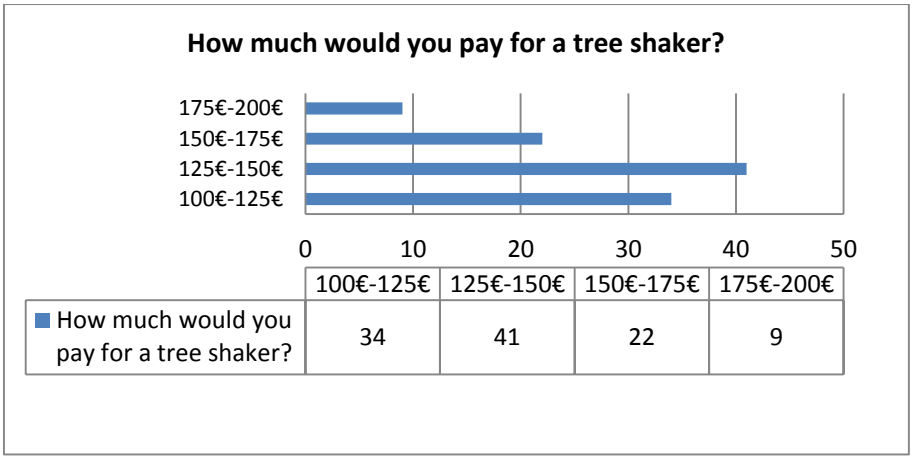

Figure 14. Selling price

7. Quality

Quality manager oversaw every parts of the tool: how much safe they are, are they satisfy the customer's requirements, etc. That is why quality manager kept connection between marketing manager and engineering designers. During the project it was suggested by the quality that battery should be built from lithium ion cells instead of buying a battery rack, because this way is cheaper and could be more ergonomic. Another suggestion was the frequency changer that helps to control the velocity of the head and the fixed head conception that is more affordable and reliable than the adjustable head. It was given tips for rod material and defined the maximum weight of the tool. Determine the maximum length of the opened and closed tool was important for carrying the tool and based on the questionnaire the price of the tool was calculated.

8. Summary

The tool was named Bosch Python, it could be a good name because the customer can memorize easily and it refers that our tool is strong.

Everybody from our group studied new technics on how to work in a group. All of the members got a lot of experience during project working, how to build-up a project, planning the steps of the project, execute the assignments and these experiences could be applied in the future works. Because of these lots of experience we would like to say thanks to the supervisors, who made this project realised. We got a bunch of suggestions and help so thanks for their work and enthusiasm.

Our group made the whole 3D model of this tool in this project work and finally you can see some pictures from the Bosch Python.

Figure 15. Bosch Python with jigsaw blade

Figure 16. Bosch Python with shaker head

9. References

[1] ZSÁRY, Á.: *Gépelemek I–II.* Tankönyvkiadó, Budapest, 1989.
[2] TERPLÁN, Z.: *Gépelemek I–II.* Nemzeti Tankönyvkiadó, Budapest.
[3] PÉTER, J.: *Géptervezés alapjai*. Miskolci Egyetemi Kiadó, Miskolc, 2008.
[4] KAMONDI, L.–SARKA, F.–TAKÁCS, Á.: *Fejlesztés-módszertani ismeretek.* Elektronikus jegyzet. TÁMOP-4.1.2-08/1/a-2009-0001, Miskolc, 2011.
[5] http://www.isixsigma.com/tools-templates/fmea/

Design of Machines and Structures, Vol. 5, No. 2 (2015) pp. 30–46.

FLOW IN CAPILLARY TUBE

JÓZSEF NAGY
Electrolux Lehel Kft.
H-5100 Jászberény, Fémnyomó u. 1.
jozsef.nagy@electrolux.hu

Abstract: In this study, I showed the equations that describe the steady state flow in the capillary in a way that no distinction should be made according to whether there is a one or a two-phase flow. This is due to the fact that the enthalpy partial derivatives in the equations are prepared by numerical calculation. In case of steady state flow I showed the throttling effect on capillary flow, as well as how to calculate (numerically) the size of the unassignable capillary flow, and the enthalpy and density of the fluid which comes into the evaporator

Keywords: *capillary, numerical simulation, steady state flow*

1. Introduction

In the cooling system of the household refrigerators the most common expansion device is the capillary tube. The capillary tube controls the amount of refrigerant flowing from the condenser to the evaporator. The capillary tube as an expansion device is used widely due to its low cost and reliable operation (no moving parts). The capillary tube as a structural component of the cooling system is one of the simplest components, but it is more difficult to understand its physical function and to describe it mathematically.

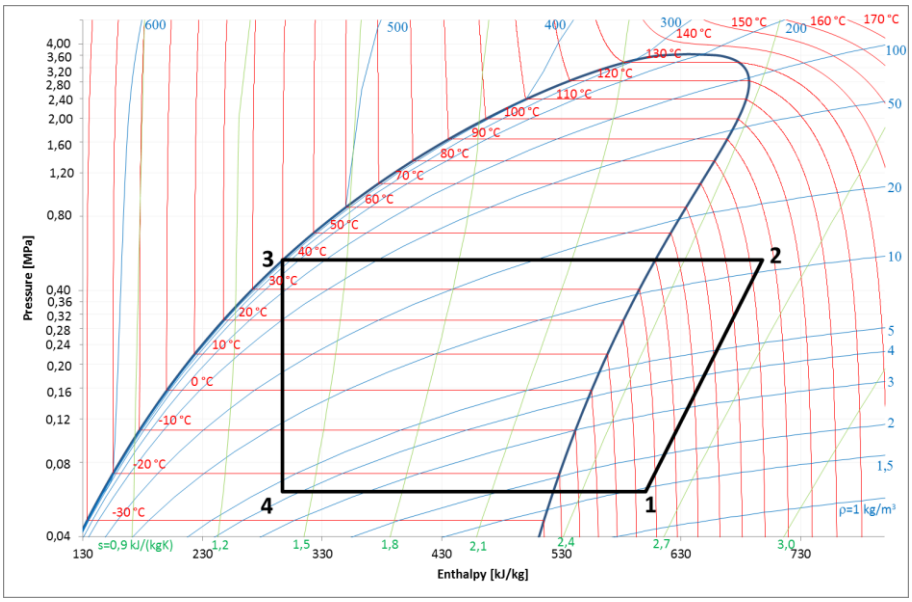

Figure 1. Theoretical cooling cycle in log(p)-h diagram

Cooling device developers determine the applicable capillary diameter and length through experiments and tests. In general, they specify the so-called capillary air flow rate. This means that they specify the amount of outgoing nitrogen volumetric flow in case of a 6 bar inlet and 1 bar outlet pressure ratio. . This value is usually given in litre/minute.

Capillary tubes are usually made of copper or aluminium. Their external diameter is 1,85 mm and the internal diameter range is 0,57; 0,63; 0,70; 0,76 mm (0,0225; 0,025; 0,0275; 0,030”). They select from this inner diameter range, and set the different air flow rate value by preparing the length of the capillary tube to the proper value.

Figure 1 shows a theoretical cooling cycle in a log(p)-h diagram. (Usually this kind of diagram is used to describe cooling cycles.) In this figure point 3 is the end of the condenser and point 4 is the front of the evaporator. These two points are connected by the capillary tube. In the theoretical cooling cycle it is assumed that the refrigerant flows from the condenser to the evaporator at a constant enthalpy (with a so called throttling state change).

In practice, the capillary tube and the suction tube, which latter connects the evaporator to the compressor, are counter flow heat exchangers. (It further complicates the description of the operation of the capillary.) Figure 2 shows this layout. The total length of the capillary is , the length of it before the heat exchanger is, the length of the heat exchanger is, the length of the capillary after the heat exchanger is which is in the insulating PUR foam. This section, therefore, we can take adiabatic.

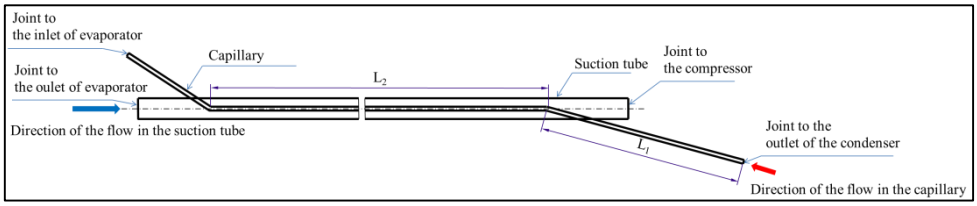

Figure 2. Structure of heat exchanger

We know what pressure (temperature) and density the medium has which enters the capillaries, but we do not know its quantity. (What is the mass flow rate?) We do not know the density (the amount of steam) and the enthalpy of the fluid, which exits the capillary and enters the evaporator. This is important to recognize so that we can tell what long evaporator is needed (or what is the size of its surface) for the entering amount of refrigerant to evaporate.

2. Equations describing the flow

Using the nominations of Figure 3 the following equation can be prescribed.

– Continuity equation

$$\frac{\partial \rho}{\partial t} + w\frac{\partial \rho}{\partial x} + \rho\frac{\partial w}{\partial x} = 0 \tag{1}$$

– Equation of motion (Euler Equation of motion)

$$\frac{\partial w}{\partial t} + w\frac{\partial w}{\partial x} + \frac{1}{\rho}\frac{\partial p}{\partial x} = -\frac{\lambda}{2D}w|w| - g\sin\alpha \tag{2}$$

– Energy equation

$$\frac{\partial h}{\partial t} + w\frac{\partial h}{\partial x} - \frac{1}{\rho}\frac{\partial p}{\partial t} + w\frac{\partial w}{\partial t} + w^2\frac{\partial w}{\partial x} = \frac{4k}{D\rho}\left(T_k - T\right) - wg\sin\alpha \tag{3}$$

– Equations of state

– Thermal equation of state

$$p = p(\rho, T) \tag{4}$$

– Caloric equation of state

$$h = h(\rho, T) \tag{5}$$

$$s = s(\rho, T) \tag{6}$$

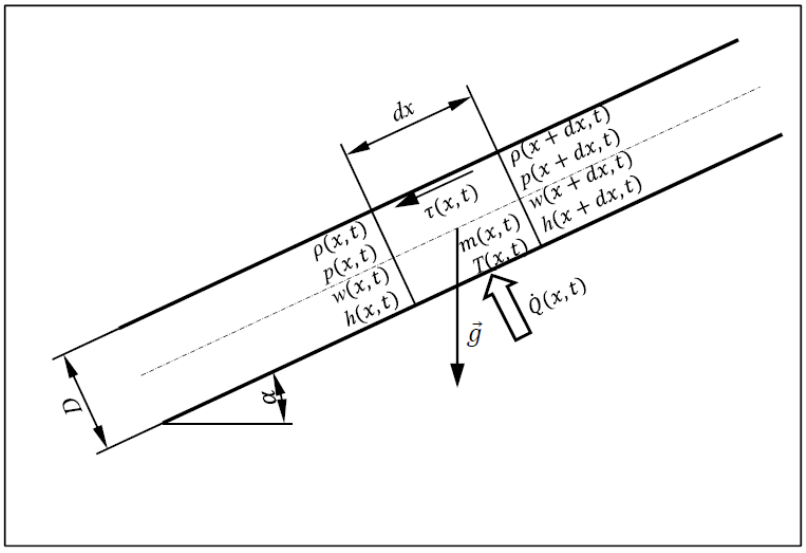

Figure 3. Elementary section of pipe with markings

– Equations for steady-state flow

In case of equations of the stationary (time constant) flow the partial derivatives of the time $\left(\frac{\partial}{\partial t}\right)$ disappear. The equations are as follows.

Continuity equation

$$\frac{\partial(\rho w)}{\partial x}=0 \quad , \tag{7}$$

this means that

$$\rho w = G = Cons \quad . \tag{8}$$

Equation of motion (Euler Equation of motion)

$$w\frac{\partial w}{\partial x}+\frac{1}{\rho}\frac{\partial p}{\partial x}=-\frac{\lambda}{2D}w|w|-g\sin\alpha \tag{9}$$

$$\underbrace{w\rho}_{G}\frac{\partial w}{\partial x}+\frac{\partial p}{\partial x}=-\frac{\lambda}{2D}\underbrace{\rho w}_{G}|w|-g\rho\sin\alpha \tag{10}$$

Energy equation

$$\frac{\partial h}{\partial x}+w\frac{\partial w}{\partial x}=\frac{4k}{D\rho w}(T_k-T)-g\sin\alpha \tag{11}$$

$$\frac{\partial h}{\partial x}+\frac{\partial\left(\frac{w^2}{2}\right)}{\partial x}=\frac{4k}{D\underbrace{\rho w}_{G}}(T_k-T)-g\sin\alpha \tag{12}$$

Equations of state are not changed.

Switching over from differentials to differences in equations (10) and (12) we get the following equations:

$$Gdw+dp=-\left(\frac{\lambda}{2D}\frac{G^2}{\rho}+g\rho\sin\alpha\right)dx \tag{13}$$

$$d\left(h+\frac{w^2}{2}\right)=\left(\frac{4k}{DG}(T_k-T)-g\sin\alpha\right)dx \quad . \tag{14}$$

$$G\Delta w+\Delta p=-\left(\frac{\lambda}{2D}\frac{G^2}{\rho}+g\rho\sin\alpha\right)\Delta x \tag{15}$$

$$\Delta\left(h+\frac{w^2}{2}\right)=\left(\frac{4k}{DG}(T_k-T)-g\sin\alpha\right)\Delta x \tag{16}$$

at the same time based on equation (8) we know that

$$w=\frac{G}{\rho} \quad . \tag{17}$$

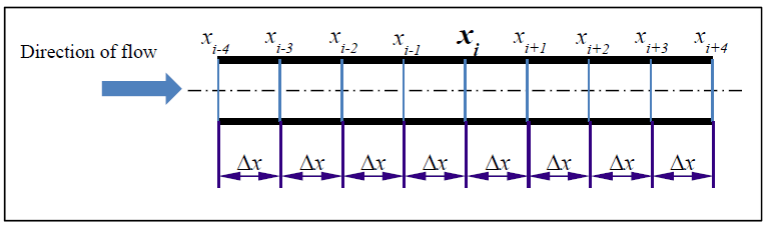

Figure 4. Net with equal scale interval

Thus, equations (15) and (16) can be written as follows (Figure 4):

$$G\left(w_{i+1}-w_i\right)+p_{i+1}-p_i=-\left(\frac{\lambda_i}{2D}\frac{G^2}{\rho_i}+g\rho_i\sin\alpha_i\right)\Delta x \tag{18}$$

$$h_{i+1}-h_i+\frac{w_{i+1}^2}{2}-\frac{w_i^2}{2}=\left(\frac{4k_i}{DG}\left(T_k-T_i\right)-g\sin\alpha_i\right)\Delta x \tag{19}$$

Taking relationship (17) into account and after rearranging (18) and (19) we get

$$p_{i+1}=-\left(\frac{\lambda_i}{2D}\frac{G^2}{\rho_i}+g\rho_i\sin\alpha_i\right)\Delta x+p_i+Gw_i-\frac{G^2}{\rho_{i+1}} \tag{20}$$

$$h_{i+1}=\left(\frac{4k_i}{DG}\left(T_k-T_i\right)-g\sin\alpha_i\right)\Delta x+h_i+\frac{w_i^2}{2}-\frac{G^2}{2\rho_{i+1}^2} \tag{21}$$

expressions. At the same time, also the caloric state equation must be satisfied i.e.

$$h_{i+1}=h\left(p_{i+1},\rho_{i+1}\right). \tag{22}$$

Equations (21) and (22) shall be equal, the pressure (p_{i+1}), calculated from relation (20), must be solved numerically concerning the density (ρ_{i+1}). It has to be solved in case of all the elementary section of pipe (Δx) under a given mass flow (G). This means that an implicit equation with high computational demands has to be solved in case of all the elementary section of pipe.

We present another option, which makes the calculations explicit (and faster). To do this refer to equations (13) and (14), and based on relation (17) express dw:

$$dw=d\left(\frac{G}{\rho}\right)=Gd\left(\frac{1}{\rho}\right)=-\frac{G}{\rho^2}d\rho \tag{1}$$

.

Substituting relation (23) into equations (13) and (14), we get the followings:

$$dp=-\left(\frac{\lambda}{2D}\frac{G^2}{\rho}+g\rho\sin\alpha\right)dx+\frac{G^2}{\rho^2}d\rho \tag{2}$$

$$dh=\left(\frac{4k}{DG}\left(T_k-T\right)-g\sin\alpha\right)dx+\frac{G^2}{\rho^3}d\rho \tag{3}$$

In addition to the independent variable dx the unknown variables are dh, dp and the dρ. We have three unknowns and two equations. The equation of state of fluid is missing. Let's make the equation of state of the fluid known numerically in h = h(p, ρ) form. From it dh can be expressed as follows:

$$dh=\left.\frac{\partial h}{\partial p}\right|_{\rho}dp+\left.\frac{\partial h}{\partial \rho}\right|_{p}d\rho \tag{4}$$

Substituting formula (26) into equation (25), we get the following relationship:

$$\left.\frac{\partial h}{\partial p}\right|_{\rho}dp=\left(\frac{4k}{DG}\left(T_k-T\right)-g\sin\alpha\right)dx+\left(\frac{G^2}{\rho^3}-\left.\frac{\partial h}{\partial \rho}\right|_{p}\right)d\rho \tag{5}$$

.

From equations (24) and (27) we get the elemental density change

$$d\rho = \frac{\left(\frac{4k}{DG}(T_k - T) - g\sin\alpha\right)dx + \left.\frac{\partial h}{\partial p}\right|_{\rho}\left(\frac{\lambda}{2D}\frac{G^2}{\rho} + g\rho\sin\alpha\right)dx}{\left.\frac{\partial h}{\partial p}\right|_{\rho}\frac{G^2}{\rho^2} + \left.\frac{\partial h}{\partial \rho}\right|_{p} - \frac{G^2}{\rho^3}} \tag{6}$$

.

Switching over to differences, the density change, the pressure change and the enthalpy change can be calculated as follows:

$$\Delta\rho_i = \frac{\left(\frac{4k_i}{DG}(T_k - T_i) - g\sin\alpha_i\right)\Delta x + \left.\frac{\partial h}{\partial p}\right|_{\rho i}\left(\frac{\lambda_i}{2D}\frac{G^2}{\rho_i} + g\rho_i\sin\alpha_i\right)\Delta x}{\left.\frac{\partial h}{\partial p}\right|_{\rho i}\frac{G^2}{\rho_i^2} + \left.\frac{\partial h}{\partial \rho}\right|_{pi} - \frac{G^2}{\rho_i^3}} \tag{29}$$

,

$$\Delta p_i = -\left(\frac{\lambda_i}{2D}\frac{G^2}{\rho_i} + g\rho_i\sin\alpha_i\right)\Delta x + \frac{G^2}{\rho_i^2}\Delta\rho_i \tag{30}$$

,

$$\Delta h_i = \left(\frac{4k_i}{DG}(T_k - T_i) - g\sin\alpha_i\right)\Delta x + \frac{G^2}{\rho_i^3}\Delta\rho_i \tag{31}$$

.

Knowing this the followings can be calculated:

$$\rho_{i+1} = \rho_i + \Delta\rho \tag{32}$$

,

$$p_{i+1} = p_i + \Delta p \tag{33}$$

,

$$h_{i+1} = h_i + \Delta h \tag{34}$$

.

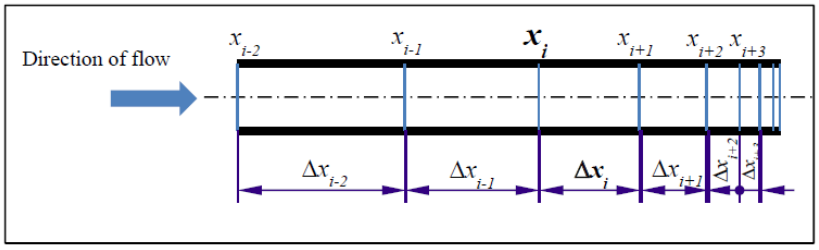

Figure 5. Net with variable scale interval

If we take Δp as independent variable, then we get the following relation for Δx_i (Figure 5) based on equations (29) and (30):

$$\Delta x_i = \frac{\left(\left.\frac{\partial h}{\partial p}\right|_{\rho i} + \frac{\rho_i^2}{G^2}\left.\frac{\partial h}{\partial \rho}\right|_{pi} - \frac{1}{\rho_i}\right)\Delta p}{\left(\frac{1}{\rho_i} - \frac{\rho_i^2}{G^2}\left.\frac{\partial h}{\partial \rho}\right|_{pi}\right)\left(\frac{\lambda_i}{2D}\frac{G^2}{\rho_i} + g\rho_i\sin\alpha_i\right) + \frac{4k_i}{DG}(T_k - T_i) - g\sin\alpha_i} \tag{35}$$

.

Δx calculated from expression (35) must be met the

$$\Delta x \geq 0 \tag{36}$$

condition. The borderline case $(\Delta x = 0)$ is met when

$$\left.\frac{\partial h}{\partial p}\right|_{\rho} + \frac{\rho^2}{G^2}\left.\frac{\partial h}{\partial \rho}\right|_{p} - \frac{1}{\rho} = 0 \tag{37}$$

equality is fulfilled. To analyse this relationship let's use the following based on expression (8)

$$\frac{\rho^2}{G^2} = \frac{1}{w^2}, \tag{38}$$

furthermore, we know the pressure, the enthalpy and the entropy as function of temperature and density based on equations (4), (5) and (6). Thus, we can write that

$$dp = \left.\frac{\partial p}{\partial \rho}\right|_{T} d\rho + \left.\frac{\partial p}{\partial T}\right|_{\rho} dT, \tag{39}$$

$$dh = \left.\frac{\partial h}{\partial \rho}\right|_{T} d\rho + \left.\frac{\partial h}{\partial T}\right|_{\rho} dT, \tag{40}$$

$$ds = \left.\frac{\partial s}{\partial \rho}\right|_{T} d\rho + \left.\frac{\partial s}{\partial T}\right|_{\rho} dT. \tag{41}$$

In equation (37) coefficients $\left.\frac{\partial h}{\partial p}\right|_{\rho}$ and $\left.\frac{\partial h}{\partial \rho}\right|_{p}$ can be expressed as follows, knowing that

$$\begin{aligned} dh &= \left.\frac{\partial h}{\partial p}\right|_{\rho} \underbrace{dp}_{\left.\frac{\partial p}{\partial \rho}\right|_{T} d\rho + \left.\frac{\partial p}{\partial T}\right|_{\rho} dT} + \left.\frac{\partial h}{\partial \rho}\right|_{p} d\rho = \\ &= \left(\left.\frac{\partial h}{\partial p}\right|_{\rho}\left.\frac{\partial p}{\partial \rho}\right|_{T} + \left.\frac{\partial h}{\partial \rho}\right|_{p}\right)d\rho + \left.\frac{\partial h}{\partial p}\right|_{\rho}\left.\frac{\partial p}{\partial T}\right|_{\rho} dT = \left.\frac{\partial h}{\partial \rho}\right|_{T} d\rho + \left.\frac{\partial h}{\partial T}\right|_{\rho} dT \end{aligned} \tag{42}$$

and relation (42) is true at any dρ and at any dT, so

$$\left.\frac{\partial h}{\partial p}\right|_{\rho}\left.\frac{\partial p}{\partial \rho}\right|_{T} + \left.\frac{\partial h}{\partial \rho}\right|_{p} = \left.\frac{\partial h}{\partial \rho}\right|_{T}, \tag{43}$$

$$\left.\frac{\partial h}{\partial p}\right|_{\rho}\left.\frac{\partial p}{\partial T}\right|_{\rho} = \left.\frac{\partial h}{\partial T}\right|_{\rho}. \tag{44}$$

Expressing coefficients $\left.\frac{\partial h}{\partial p}\right|_{\rho}$ and $\left.\frac{\partial h}{\partial \rho}\right|_{p}$ from relations (43) and (44)

$$\left.\frac{\partial h}{\partial p}\right|_{\rho} = \frac{\left.\frac{\partial h}{\partial T}\right|_{\rho}}{\left.\frac{\partial p}{\partial T}\right|_{\rho}}, \tag{45}$$

$$\left.\frac{\partial h}{\partial \rho}\right|_{p} = \left.\frac{\partial h}{\partial \rho}\right|_{T} - \frac{\left.\frac{\partial h}{\partial T}\right|_{\rho}}{\left.\frac{\partial p}{\partial T}\right|_{\rho}} \left.\frac{\partial p}{\partial \rho}\right|_{T}, \tag{46}$$

and substituting them into equation (37) we get

$$\frac{\left.\frac{\partial h}{\partial T}\right|_{\rho}}{\left.\frac{\partial p}{\partial T}\right|_{\rho}} + \frac{1}{w^2}\left(\left.\frac{\partial h}{\partial \rho}\right|_{T} - \frac{\left.\frac{\partial h}{\partial T}\right|_{\rho}}{\left.\frac{\partial p}{\partial T}\right|_{\rho}} \left.\frac{\partial p}{\partial \rho}\right|_{T}\right) - \frac{1}{\rho} = 0 \tag{47}$$

.

Write the first law of thermodynamics in the

$$dh - \frac{dp}{\rho} = Tds \tag{48}$$

form and using relations (39), (40) and (41), we can write

$$\left.\frac{\partial h}{\partial \rho}\right|_{T} d\rho + \left.\frac{\partial h}{\partial T}\right|_{\rho} dT - \frac{1}{\rho}\left.\frac{\partial p}{\partial \rho}\right|_{T} d\rho - \frac{1}{\rho}\left.\frac{\partial p}{\partial T}\right|_{\rho} dT = T\left.\frac{\partial s}{\partial \rho}\right|_{T} d\rho + T\left.\frac{\partial s}{\partial T}\right|_{\rho} dT \tag{49}$$

.

Equation (49) must be fulfilled at each dρ and dT, therefore

$$\left.\frac{\partial h}{\partial \rho}\right|_{T} - \frac{1}{\rho}\left.\frac{\partial p}{\partial \rho}\right|_{T} = T\left.\frac{\partial s}{\partial \rho}\right|_{T}, \tag{50}$$

$$\left.\frac{\partial h}{\partial T}\right|_{\rho} - \frac{1}{\rho}\left.\frac{\partial p}{\partial T}\right|_{\rho} = T\left.\frac{\partial s}{\partial T}\right|_{\rho}. \tag{51}$$

.

Expressing partial derivatives $\left.\frac{\partial h}{\partial \rho}\right|_{T}$ and $\left.\frac{\partial h}{\partial T}\right|_{\rho}$ from equations (50) and (51):

$$\left.\frac{\partial h}{\partial \rho}\right|_{T} = T\left.\frac{\partial s}{\partial \rho}\right|_{T} + \frac{1}{\rho}\left.\frac{\partial p}{\partial \rho}\right|_{T}, \tag{52}$$

$$\left.\frac{\partial h}{\partial T}\right|_{\rho} = T\left.\frac{\partial s}{\partial T}\right|_{\rho} + \frac{1}{\rho}\left.\frac{\partial p}{\partial T}\right|_{\rho}, \tag{53}$$

and substituting them into equation (47)

$$\frac{T\left.\frac{\partial s}{\partial T}\right|_{\rho} + \frac{1}{\rho}\left.\frac{\partial p}{\partial T}\right|_{\rho}}{\left.\frac{\partial p}{\partial T}\right|_{\rho}} + \frac{1}{w^2}\left(T\left.\frac{\partial s}{\partial \rho}\right|_{T} + \frac{1}{\rho}\left.\frac{\partial p}{\partial \rho}\right|_{T} - \frac{T\left.\frac{\partial s}{\partial T}\right|_{\rho} + \frac{1}{\rho}\left.\frac{\partial p}{\partial T}\right|_{\rho}}{\left.\frac{\partial p}{\partial T}\right|_{\rho}} \left.\frac{\partial p}{\partial \rho}\right|_{T}\right) - \frac{1}{\rho} = 0 \tag{54}$$

,

$$\frac{T\left.\frac{\partial s}{\partial T}\right|_{\rho}}{\left.\frac{\partial p}{\partial T}\right|_{\rho}}+\frac{1}{\rho}+\frac{1}{w^2}\left(T\left.\frac{\partial s}{\partial \rho}\right|_{T}+\frac{1}{\rho}\left.\frac{\partial p}{\partial \rho}\right|_{T}-\frac{T\left.\frac{\partial s}{\partial T}\right|_{\rho}}{\left.\frac{\partial p}{\partial T}\right|_{\rho}}\left.\frac{\partial p}{\partial \rho}\right|_{T}-\frac{1}{\rho}\left.\frac{\partial p}{\partial \rho}\right|_{T}\right)-\frac{1}{\rho}=0 \tag{55}$$

,

$$\frac{T\left.\frac{\partial s}{\partial T}\right|_{\rho}}{\left.\frac{\partial p}{\partial T}\right|_{\rho}}+\frac{1}{w^2}\left(T\left.\frac{\partial s}{\partial \rho}\right|_{T}-\frac{T\left.\frac{\partial s}{\partial T}\right|_{\rho}}{\left.\frac{\partial p}{\partial T}\right|_{\rho}}\left.\frac{\partial p}{\partial \rho}\right|_{T}\right)=0 \tag{56}$$

,

$$\frac{T}{w^2\left.\frac{\partial p}{\partial T}\right|_{\rho}}\underbrace{\left(w^2\left.\frac{\partial s}{\partial T}\right|_{\rho}+\left.\frac{\partial s}{\partial \rho}\right|_{T}\left.\frac{\partial p}{\partial T}\right|_{\rho}-\left.\frac{\partial s}{\partial T}\right|_{\rho}\left.\frac{\partial p}{\partial \rho}\right|_{T}\right)}_{=0}=0 \tag{57}$$

.

It follows that

$$w^2=\left.\frac{\partial p}{\partial \rho}\right|_{T}-\frac{\left.\frac{\partial p}{\partial T}\right|_{\rho}}{\left.\frac{\partial s}{\partial T}\right|_{\rho}}\left.\frac{\partial s}{\partial \rho}\right|_{T}=\left.\frac{\partial p}{\partial \rho}\right|_{s}=a^2 \tag{58}$$

,

i.e.

$$w=a \tag{59}$$

where the speed of sound is $a=\sqrt{\left.\frac{\partial p}{\partial \rho}\right|_{s}}$.

In relation (58) the second equality can be provided as follows. Write down the pressure as the function of entropy and density, i.e. p = p(s, ρ), so in this case

$$dp=\left.\frac{\partial p}{\partial s}\right|_{\rho}ds+\left.\frac{\partial p}{\partial \rho}\right|_{s}d\rho \tag{60}$$

.

Using relations (39) and (41)

$$dp=\left(\left.\frac{\partial p}{\partial s}\right|_{\rho}\left.\frac{\partial s}{\partial \rho}\right|_{T}+\left.\frac{\partial p}{\partial \rho}\right|_{s}\right)d\rho+\left.\frac{\partial p}{\partial s}\right|_{\rho}\left.\frac{\partial s}{\partial T}\right|_{\rho}dT=\left.\frac{\partial p}{\partial \rho}\right|_{T}d\rho+\left.\frac{\partial p}{\partial T}\right|_{\rho}dT \tag{61}$$

,

$$\left.\frac{\partial p}{\partial s}\right|_{\rho}\left.\frac{\partial s}{\partial T}\right|_{\rho}=\left.\frac{\partial p}{\partial T}\right|_{\rho}\Rightarrow\left.\frac{\partial p}{\partial s}\right|_{\rho}=\frac{\left.\frac{\partial p}{\partial T}\right|_{\rho}}{\left.\frac{\partial s}{\partial T}\right|_{\rho}} \tag{62}$$

,

$$\left.\frac{\partial p}{\partial s}\right|_{\rho}\left.\frac{\partial s}{\partial \rho}\right|_{T}+\left.\frac{\partial p}{\partial \rho}\right|_{s}=\left.\frac{\partial p}{\partial \rho}\right|_{T}\Rightarrow\left.\frac{\partial p}{\partial \rho}\right|_{s}=\left.\frac{\partial p}{\partial \rho}\right|_{T}-\left.\frac{\partial p}{\partial s}\right|_{\rho}\left.\frac{\partial s}{\partial \rho}\right|_{T}=\left.\frac{\partial p}{\partial \rho}\right|_{T}-\frac{\left.\frac{\partial p}{\partial T}\right|_{\rho}}{\left.\frac{\partial s}{\partial T}\right|_{\rho}}\left.\frac{\partial s}{\partial \rho}\right|_{T} \tag{63}$$

.

In summary the $\Delta x = 0$ is satisfied if the speed is equal to the speed of sound. In addition, the condition $\Delta x = 0$ at location $x \geq L$ must be met.

When $\Delta x = 0$ (but now let's turn back to differentials and using relation $dx = 0$), then equation (10) is as follows:

$$dw = -\frac{dp}{G}, \tag{64}$$

and relation (11) is

$$dh + wdw = 0. \tag{65}$$

Rearranging it and replacing dh by relation (48) and replacing dw by expression (64) we can write

$$Tds + \frac{dp}{\rho} - \underbrace{\frac{w}{G}}_{\frac{1}{\rho}} dp = 0. \tag{66}$$

It follows that, where $\Delta x = 0$, there the change in the entropy also becomes zero ($ds = 0$), i.e., the entropy reaches its maximum. Entropy is defined by:

$$ds = \frac{\delta q}{T} \tag{67}$$

if the $\delta q \geq 0$, then the $ds \geq 0$, i.e. the entropy cannot be reduced.

If at given mass flow the speed of flow reaches the speed of sound at location $x < L$ (it is not possible), then the capillary is not able to let that mass flow rate flow through, but only a smaller mass flow rate where the speed of flow reaches the speed of sound at location $x = L$. This phenomenon is called throttling.

At the given mass flow rate $\dot{m}$ the pressure p can be calculated where the velocity reaches the speed of sound namely by the iterative solution of relationship

$$\frac{\dot{m}}{A} = G = \rho w = \rho a(\rho, p). \tag{68}$$

If the resulting pressure p is less than the evaporation pressure (p_e), then no throttling occurs. However, if the pressure value is higher than the evaporation pressure, then throttling occurs, which means that the capillary is not capable of transmitting this flow rate. Thus, the flow rate has to be determined (also in an iterative way) so that equality $w = a$ can meet at place $x = L$. The resulting mass flow must redefine the pressure at which the velocity reaches the speed of sound. The iteration has to be carried out, as long as relation (68) and equality $w = a$ simultaneously satisfies at place $x = L$. So it can determine numerically the capillary mass flow rate.

3. Numerical methods

The first step is to determine Δp. To do this, we first need to calculate the pressure value p where at a given mass flow the rate of flow reaches the speed of sound. If

this pressure is lower than the evaporation pressure, then $\Delta p = \frac{p_c - p_e}{n}$, if it is greater, then $\Delta p = \frac{p_c - p}{n}$.

To determine pressure p we must know the speed of sound, as a function of the pressure and the density. The bases of the numerical determination of the speed of sound is given by equation (63). (Details below.)

Now let's suppose that we were able to determine Δp. Thus, the next step is the calculation of Δx based on relation (35).

The determinations of coefficients in equation (35) are the followings.

1. Numerical determination of $\left.\frac{\partial h}{\partial p}\right|_{\rho}$

The bases of the numerical determination of $\left.\frac{\partial h}{\partial p}\right|_{\rho}$ gives equation(45). So we trace back $\left.\frac{\partial h}{\partial p}\right|_{\rho}$ to the numerical determination of $\left.\frac{\partial h}{\partial T}\right|_{\rho}$ and $\left.\frac{\partial p}{\partial T}\right|_{\rho}$.

According to equations (4) and (5) we know the pressure and the enthalpy as a function of the density and temperature. Here we assume the numerical knowledge of these functions.

Based on Figure 6 the numerical partial derivatives can be prepared by the following formulas:

$$\left.\frac{\partial h}{\partial T}\right|_{\rho i} = \frac{h_{i-2} - 8h_{i-1} + 8h_{i+1} - h_{i+2}}{12\Delta T} + \mathrm{O}\left((\Delta T)^4\right) \tag{69}$$

$$\left.\frac{\partial p}{\partial T}\right|_{\rho i} = \frac{p_{i-2} - 8p_{i-1} + 8p_{i+1} - p_{i+2}}{12\Delta T} + \mathrm{O}\left((\Delta T)^4\right) \tag{70}$$

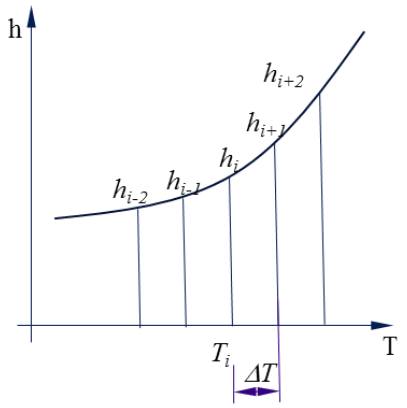

Figure 6. Numerical determination of partial derivatives

Similarly to relationships (69) and (70) we could also set $\left.\frac{\partial h}{\partial p}\right|_{\rho}$, but the pressure and the enthalpy are known as a function of temperature and density so it is appropriate to introduce partial derivatives of these variables.

Figure 7 and Figure 8 show functions $p(T)|_{\rho}$ and $h(T)|_{\rho}$ in case of isobutene (R600a).

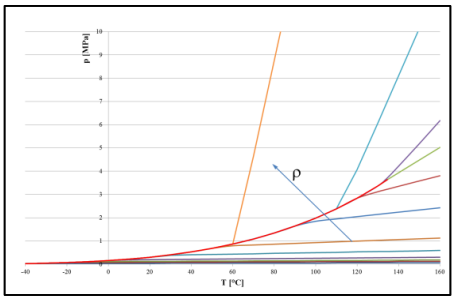

Figure 7. p(T) ρ = Constant

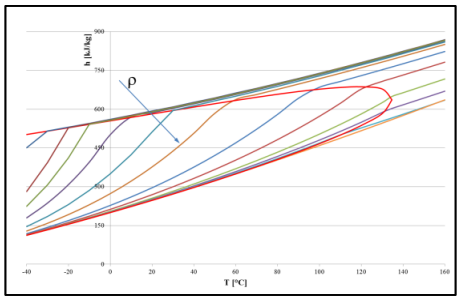

Figure 8. h(T) ρ = Constant

2. Numerical determination of $\left.\frac{\partial h}{\partial \rho}\right|_{p}$

Like in the previous point, here we also trace it back to the partial derivatives of the temperature and density. This tracing back is possible according to relation (46). In addition to the foregoing, here are also the enthalpy and pressure partial derivatives of density at a constant temperature. Numerical determination of them is possible according to the approximate relationships (71, 72). Figure 7 and Figure 8 show the functions $p(\rho)|_{T}$ and $h(\rho)|_{T}$ in case of the isobutene (R600a).

$$\left.\frac{\partial h}{\partial \rho}\right|_{T\,i} = \frac{h_{i-2} - 8h_{i-1} + 8h_{i+1} - h_{i+2}}{12\Delta\rho} + \mathrm{O}\left((\Delta\rho)^4\right) \quad (71)$$

,

$$\left.\frac{\partial p}{\partial \rho}\right|_{T\,i} = \frac{p_{i-2} - 8p_{i-1} + 8p_{i+1} - p_{i+2}}{12\Delta\rho} + \mathrm{O}\left((\Delta\rho)^4\right) \quad (72)$$

.

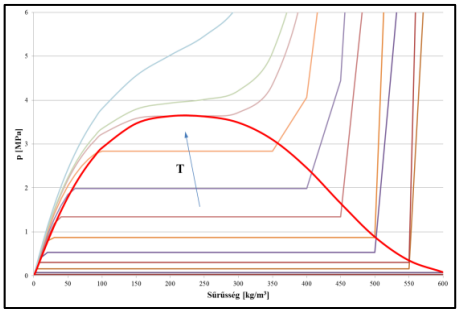

Figure 9. p(ρ) T = Constant

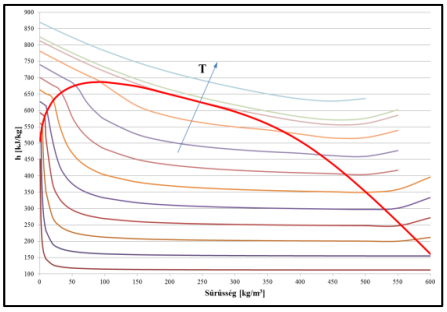

Figure 10. h(ρ) T = Constant

3. λ pipe friction factor is defined in the function of the Reynolds-number.

For two-phase in the calculation of Reynolds-number $\mathrm{Re} = \frac{Dw}{\upsilon} = \frac{DG}{\eta}$ the dynamic viscosity is considered below according to relation [13]

$$\eta = \frac{1}{\frac{x_g}{\eta_g} + \frac{1 - x_g}{\eta_f}} \quad . \tag{73}$$

Depending on the value of the Reynolds number pipe friction factor can be calculated as follows according to [17]:

if $\mathrm{Re} \leq 2320$, then in the context of laminar flow

$$\lambda = \frac{64}{\mathrm{Re}} \quad , \tag{74}$$

if $2320 < \mathrm{Re} \leq 10^5$, then

$$\lambda = 0{,}3164 \cdot \mathrm{Re}^{-0{,}25} \tag{75}$$

according to the Blasius equation,

if $10^5 < \mathrm{Re} < 10^8$, then

$$\lambda = 0{,}0032 + 0{,}221 \cdot \mathrm{Re}^{-0{,}237} \tag{76}$$

according to Nikuradse.

4. Definition of the heat transfer coefficient k

The heat transfer coefficient of the inner cylindrical wall surface has to be calculated according to the following equation [5]:

$$k_b = \frac{1}{\frac{1}{\alpha_b} + \frac{D \cdot \ln\left(\frac{D_k}{D}\right)}{2\lambda_{cső}} + \frac{D}{D_k \alpha_k}} \quad , \tag{77}$$

where $\alpha_k = 1{,}32\left(\frac{\Delta T}{D_k}\right)^{1/4}$, $\alpha_b = \frac{\lambda Nu}{D}$ can be calculated.

For a phase the Nusselt-number is calculated according to the Dittus–Boelter-equation

$$Nu = 0{,}023 \cdot \mathrm{Re}^{0{,}8}\, \mathrm{Pr}^{0{,}3} \quad , \tag{78}$$

$$\mathrm{Pr} = \frac{c_p \eta}{\lambda_h} \quad . \tag{79}$$

For two-phases [7]:

$$Nu = \frac{\alpha_b D}{\lambda_{hf}} = 0{,}026 \cdot \mathrm{Re}_m^{0{,}8}\, \mathrm{Pr}_f^{1/3} \quad , \tag{80}$$

where (m: mixture)

$$\mathrm{Re}_m = \frac{Dw}{\eta_f}\left[\rho_f + \rho_g\left(\frac{\rho_f}{\rho_g}\right)^{1/2}\right]. \tag{81}$$

5. Determination of the partial derivative $\left.\frac{\partial p}{\partial \rho}\right|_s$ for the calculation of the speed of sound

We also trace it back to the partial derivatives of the temperature and density, according to relation

$$\left.\frac{\partial p}{\partial \rho}\right|_s = \left.\frac{\partial p}{\partial \rho}\right|_T - \frac{\left.\frac{\partial p}{\partial T}\right|_\rho}{\left.\frac{\partial s}{\partial T}\right|_\rho}\left.\frac{\partial s}{\partial \rho}\right|_T. \tag{82}$$

$\left.\frac{\partial p}{\partial \rho}\right|_T$ can be calculated based on the (72), and $\left.\frac{\partial p}{\partial T}\right|_\rho$ based on the approximation (70).

Similarly, the missing partial derivatives can be determined using expressions (83, 84) and with the help of Figure 11 and Figure 12.

$$\left.\frac{\partial s}{\partial T}\right|_{\rho i} = \frac{s_{i-2} - 8s_{i-1} + 8s_{i+1} - s_{i+2}}{12\Delta T} + \mathrm{O}\left((\Delta T)^4\right), \tag{83}$$

$$\left.\frac{\partial s}{\partial \rho}\right|_{T i} = \frac{s_{i-2} - 8s_{i-1} + 8s_{i+1} - s_{i+2}}{12\Delta \rho} + \mathrm{O}\left((\Delta \rho)^4\right). \tag{84}$$

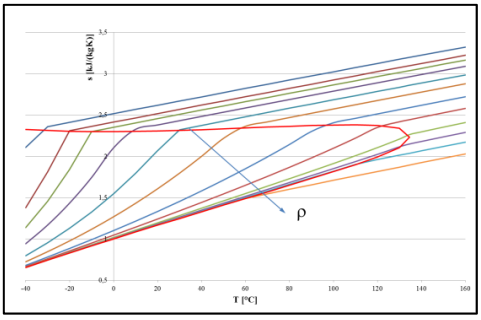

Figure 11. s(T) ρ = Constant

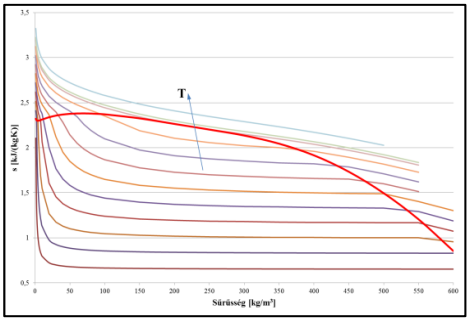

Figure 12. s(ρ) T = Constant

4. Results

Knowing the state surfaces of the fluid according to relation (4), (5) and (6) we can calculate the pressure, the density, the enthalpy and the velocity as a function of location. In addition, we can calculate how much mass flow the given geometry

capillary is capable to transmit through knowing the pressure, density and enthalpy of the entering fluid.

If the fluid is nitrogen, then the capillary airflow rate can be determined by calculation, as well as the length of the capillary needed to achieve the desired airflow rate at a selected inside diameter of the pipe.

Figure 1 shows a theoretical cooling cycle in log(p)-h chart. It is theoretical, because the capillary flow assumes a constant enthalpy (between points 3 and 4) and the compressor presses the refrigerant into the condenser at constant entropy (between points 1 and 2). This study does not deal with the compressor. This study deals with the flow between points 3 and 4, and we are particularly interested in the flow around point 4.

Let's take a look at how to develop the flow in the capillary tube under the following assumptions:

The inner diameter of the capillary is 0,7 mm, its total length (L) is 2800 mm, the length before the heat exchanger (L_1) is 380 mm, the length of the heat exchanger (L_2) is 1330 mm.

The temperature of the refrigerant (R600a) in the condenser is 40°C, and it is a saturated liquid.

The temperature of the fluid in the evaporator is –24°C.

On the length before the heat exchanger (L_1) the capillary tube is in contact with the static ambient air, having a temperature of 25°C.

On the heat exchanger section the air temperature varies linearly between –20°C and +10°C around the capillary.

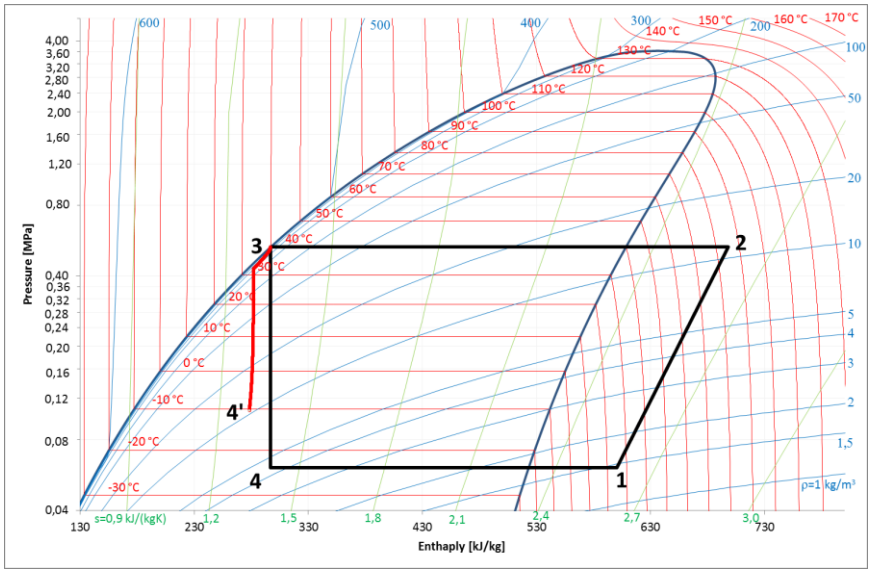

Figure 13. The pressure in capillary as a function of the enthalpy

After the heat exchanger, the capillary is in the insulating foam (PU foam). This section is considered to be adiabatic.

The resulting pressure in the capillary is marked on Figure 13 with a thick red curve (between points 3 and 4) in a log(p)-h chart. It can be seen that the capillary pressure is higher at end than the pressure in the evaporator (point 4). This also means that throttling occurs. The capillary is capable of transmitting a 1,278593 kg/h mass flow under the above conditions. The pressure is 0,106859 MPa at the end of the capillary, which corresponds to a 10,3048°C fluid.

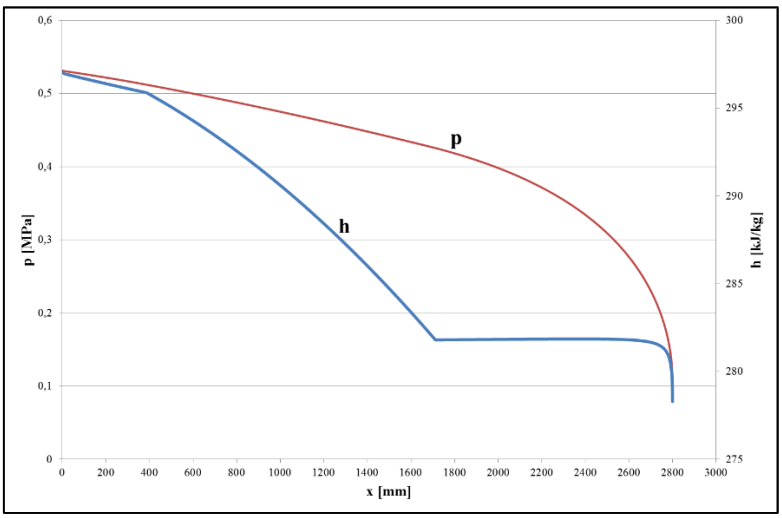

Figure 14. h(x) and p(x) in the capillary

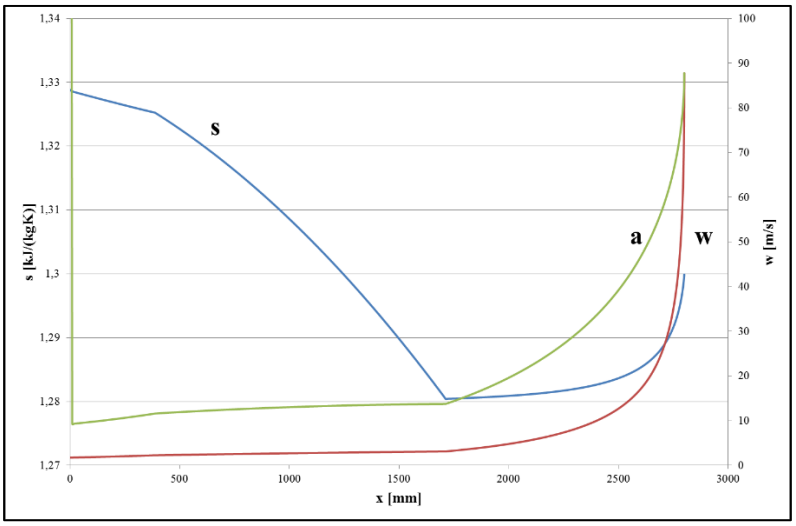

Figure 15. s(x), w(x) and a(x) in the capillary

5. Summary

In this study, I showed the equations that describe the steady state flow in the capillary in a way that no distinction should be made according to whether there is a one or a two-phase flow. This is due to the fact that the enthalpy partial derivatives in the equations are prepared by numerical calculation.

In case of steady state flow I showed the throttling effect on capillary flow, as well as how to calculate (numerically) the size of the unassignable capillary flow, and the enthalpy and density of the fluid which comes into the evaporator. With that I have answered the questions asked in the first part.

6. References

[1] CZIBERE, Tibor: *Vezetéses hőátvitel*. Miskolci Egyetemi Kiadó, Miskolc, 1998.
[2] JAKAB, Zoltán: *Kompresszoros hűtés I–II*. Magyar Mediprint Szakkiadó Kft.
[3] JAKAB, Zoltán: *Háztartási hűtőbútorok és komfort léghűtők*. 2. javított kiadás. Hűtő- és Klímatechnikai Vállalkozások Szövetsége, 2006.
[4] GAÁL, Ferenc: *Kishűtőgépek*. Műszaki Könyvkiadó, 1972.
[5] HOLMAN, J. P.: *Heat transfer. 7th Edition in SI Units*. McGrow-Hill Book Company, 1992.
[6] ULLRICH, Hans-Jürgen: *Hűtőtechnika I.* Soós és Társa Hűtőtechnikai Rt., 1999.
[7] ARORA, C. P.: *Refrigeration and air conditioning*. 3rd edition. Tata McGraw Hill Education Private Limited, 2010.
[8] REYNOLDS, W. C.: *Thermodynamic properties in SI graphs, tables, and computational equations for 40 substances*. Department of Machanical Engineering Stanford University, 1979.
[9] CARLSLAW, H. S.–JAEGER, J. C.: *Conduction of heat in solids*. 2nd edition. Oxford University Press, 1959.
[10] SZABÓ, Szilárd: *Erő- és munkagépek.* Előadásvázlat.
[11] SZABÓ, Szilárd: *Gázdinamika*. Előadásvázlat.
[12] KALMÁR, L.–BARANYI, L.: *Hő- és áramlástani feladatok numerikus modellezése*. Szakmérnöki jegyzet. Miskolci Egyetem, Miskolc, 2006.
[13] HUHN, J.–WOLF, J.: *Kétfázisú áramlás. Gáz-folyadék rendszerek*. Műszaki Könyvkiadó, Budapest, 1978.
[14] GARBAI, L.–DEZSŐ, Gy.: *Áramlás energetikai csővezetékrendszerekben*. Műszaki Könyvkiadó, Budapest, 1986.
[15] VIDA, Gy.: *Műszaki hőtan*. Tankönyvkiadó, Budapest, 1991.
[16] ZHANG, C. L.–DING, G. L.: Approximate analytic solutions of adiabatic capillary tube. *International Journal of Refrigeration*, 2004 (27), 17–24.
[17] CZIBERE, Tibor: *Áramlástan*. Tankönyvkiadó, Budapest, 1990.

Design of Machines and Structures, Vol. 5, No. 2 (2015) pp. 47–54.

MEASURING METHOD TO DETERMINE THE VIBRATION DAMPING BEHAVIOUR OF METALLIC FOAMS

FERENC SARKA–ÁDÁM DÖBRÖCZÖNI–ATTILA SZILÁGYI
University of Miskolc, H-3515 Miskolc-Egyetemváros, Hungary
machsf@uni-miskolc.hu

Abstract: In this paper the authors describe a measuring method to determine the vibration damping behaviour of the metallic foams and try to determine which damping model is good to describe the behaviour of metallic foams (Coulomb damping or viscous damping).

Keywords: *metallic foams, vibration damping, damping model*

1. Introduction

The technological development brought close to avail metallic foams for designers in industrial use. Many Hungarian institutions are manufacturing and working with metallic foams such as the University of Miskolc and the Bay Zoltán Nonprofit Ltd. in Miskolc, or in Budapest the Budapest University of Technology and Economics.

The name metallic foam indicates such a solid metallic material, which has more than 90% porosity (some manufacturer produces 'metal foams' less than 90% porosity). The density of this kind of materials is less by one order of magnitude. Metallic foam has several properties that make its use desirable in engineering. These properties are energy-absorbing, heat conduction, damping, sound-absorbing and filtering abilities. Metallic foams have two types; the open-cell and closed-cell ones. Most of the cases the material of the metallic foam is aluminium-alloy but metallic foam also can be created from other materials (steel, copper, silver and titan) [1], [2].

Many researches were carried out to determine physical, chemical and mechanical properties of metallic foams. Properties of metallic foams depend on the size of the cells, the thickness of the walls (bridges) between the cells and the shape of the cells if the material is the same. With the use of the modified ratio between the solid metal density and the foam metal density, we can approximately determine foam material properties. The computational equation is equation (1).

$$\frac{P}{P^0} = k \cdot \left(\frac{\rho}{\rho^0} \right)^n \tag{1}$$

where,
P: a kind of property,
ρ: density,
0: index for metals, without index 0 is for metal foams,
n, k: can be chosen according to Table 1, parameters from measurements.

Literature is short-spoken in the point of view of the damping behaviour of metallic foams. About the damping behaviour of solid metals many literature publish data such as logarithmical decrement or Lehr's damping ratio [3], [4].

That would be obvious to use equation (1) to determine the damping capability of metallic foams. The damping capability of metallic foams is worse than for the solid metal materials will be the result if we make the calculation. This would be the opposite of those statements that underline the significant vibration damping capability of metallic foams. We can determine that equation (1) cannot use for determine vibration damping capability of metallic foams.

Table 1
k and n factors to determine parameters of metal foams

Property	**k**	**n**
R (Ωm)	1	–1.6÷–1.85
λ (W/mK)	1	1.6÷1.85
E (GPa)	0.1÷4	1.8÷2.2
σ (MPa)	0÷1.0	1.5÷2

Literature is short-spoken in the point of view of the damping behaviour of metallic foams. About the damping behaviour of solid metals many literature publish data such as logarithmical decrement or Lehr's damping ratio [3], [4].

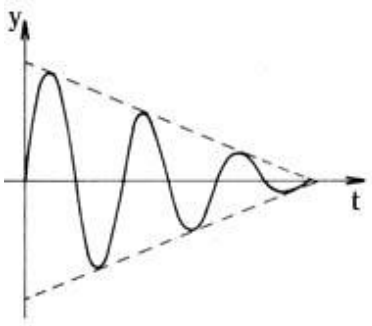

Figure 1. Nature and the envelope of Coulomb damping

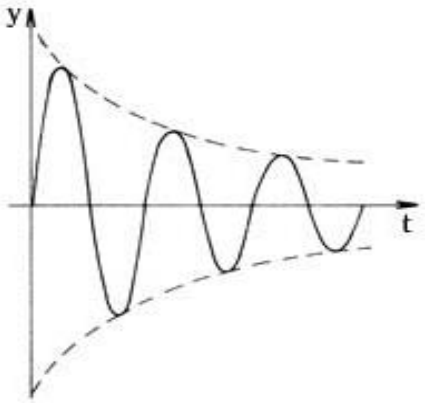

Figure 2. Nature and the envelope of viscous damping

That would be obvious to use equation (1) to determine the damping capability of metallic foams. The damping capability of metallic foams is worse than for the solid metal materials will be the result if we make the calculation. This would be the opposite of those statements that underline the significant vibration damping capability of metallic foams. We can determine that equation (1) cannot use for determine vibration damping capability of metallic foams.

Vibration damping behaviour of solid metal materials can be described with a viscous damping model (Figure 2). It is questionable whether we can use or not the same damping model for metallic foams.

Next chapters will be described a measurement, which can help to determine the vibration damping behaviour of metallic foams and the value of logarithmical decrement. This paper introduces the next step of the research introduced in [1].

2. Shape of the sample and the layout of the measurement

We made beams with rectangular cross-section from the metallic foam material. The beam was made from a greater metallic foam plate with a milling machine.

Figure 3. The metallic foam beam

The dimensions of the metallic foam beam: 35.5 mm x 27 mm x 300 mm, weight 92 g (Figure 3). We fastened a weight to one of the ends of the beam with a screw fastening (it is signed with m0 in Figure 6), in this way set up the sample (Figure 4).

Figure 4. The sample

We fastened the free end of the assembled sample with a fixed support (Figure 5).

Figure 5. Fasten of the sample

We placed load to the sample with another weight, with a help of a fishing line (signed with m in Figure 6). After cutting the fishing line which held the (m) weight we measured the displacement of the free end of the beam. The displacement was measured with a laser displacement meter (signed with L in Figure 6). The sketch of the measurement can be seen in Figure 6, and real measuring in Figure 7.

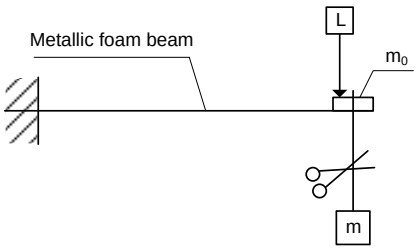

Figure 6. Sketch of the measurement

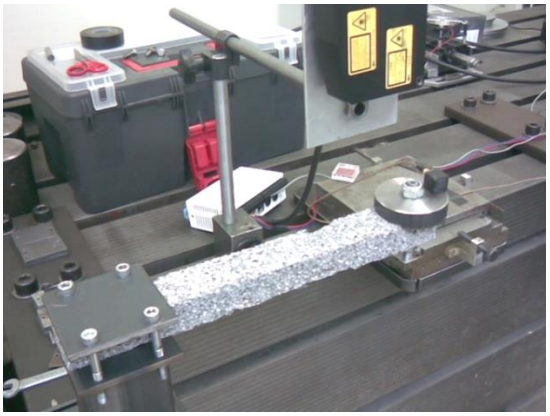

Figure 7. Real environment of the measurement

We lead the fishing line of the weight trough the bore in the fasten screw of the m0 weight. We chose this type of line leading to prevent the sample to make vibration outside the vertical plain. Measurements were made with 1 kg, 2 kg, 3 kg loads. Beside the measurements with loads, we made knocking measurements too. We compared the two types of measurement.

3. Measured data

We saw the displacement of the free end of the metallic foam beam on the computer monitor. A picture from the computer monitor can be seen in Figure 8.

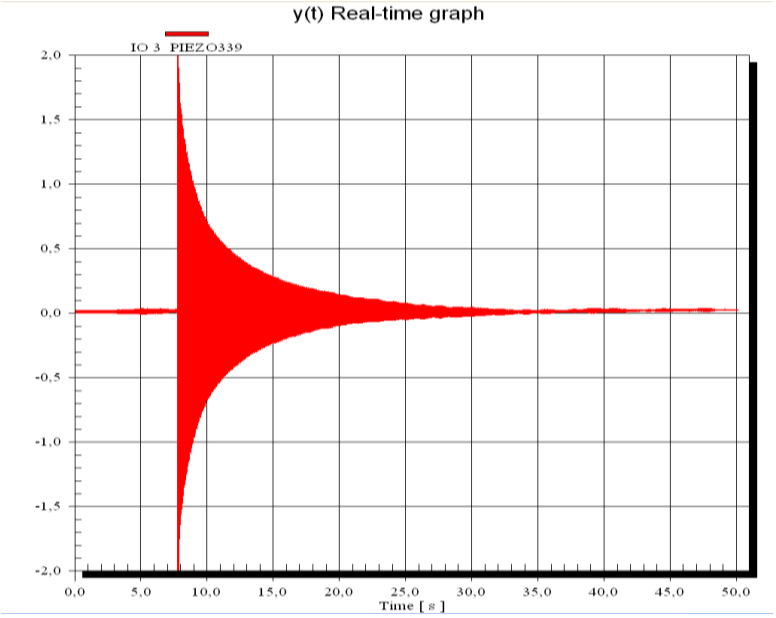

Figure 8. Displacement of the end of the beam depending on time

The measurement software is able to export the measured data into Excel format. Further processing was made in Microsoft™ Excel™. Excel file contains the measured data (displacements) in one column. We need to modify the measured displacement data to get result from that.

Modifications were the following:

- remove data before the line was cut,
- remove data after the vibration ends,
- place the curve symmetrical to the abscissa.

After modification, we received such a curve, where we could determine the logarithmical decrement. After the analysis, we experienced that the value of the logarithmical decrement was not permanent during the vibration. According to the results we concluded that the damping behaviour of the metallic foams is not the classical viscous damping type. The curve does not fit to the Coulomb type damping,

where the damping coefficient is increasing with the vibration time. This symptom leaded us to carry on to analysing the measured data. We made other modifications on the measured data. We filtered the peak values of the vibration wave and used just the positive values.

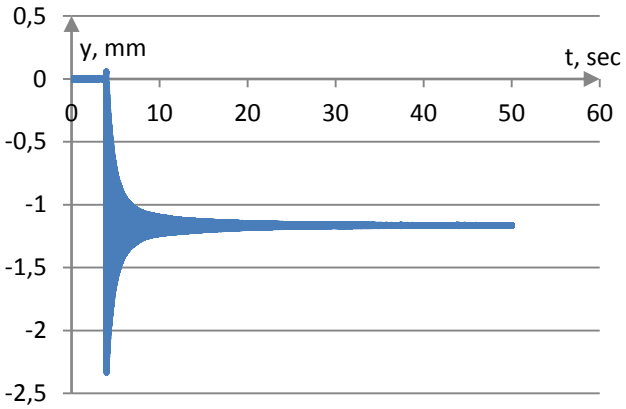

Figure 9. Displacement of the rod end after the line was cut (1 kg load)

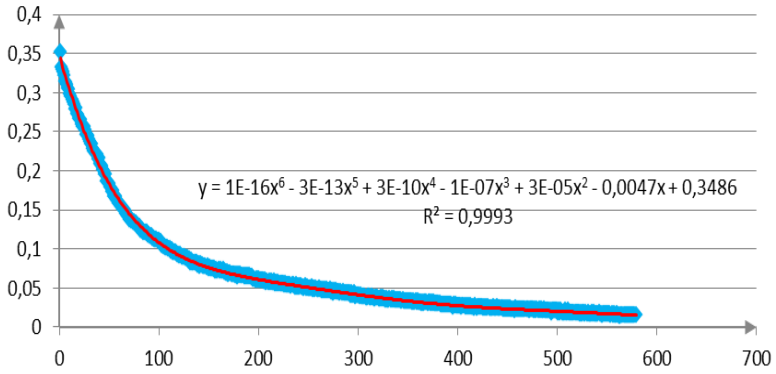

Figure 10. The diagram shows the positive amplitudes (abscissa: number of positive peaks, ordinate: the value of the peak in mm)

In Figure 10 the curve generated by points of positive amplitudes of the vibration can be seen. The figure also shows the trend line of the curve and the determination coefficient (R2). The equation of the trend line also can be seen in Figure 10, which is a sixth grade polynomial. The value of the determination coefficient is almost 1, that is to say it is a good approximation. This is not fit nor to Coulomb type damping nor to viscous damping. If we observe Figure 10, approximately at the 70th peak, the curve of the trend line suddenly turns aside. We divided the curve into two parts, and examined them separately. The first part of the curve can be seen in Figure 11. We placed a new trend line to the curve of Figure 11. In Figure 11 the equation of the

trend line and the determination coefficient also can be seen. The approximation of the point is good, because the R2 is 0.9915.

The curve of Figure 11 is almost line, which is continuously decreasing. This type of envelope is the type of the Coulomb damping envelope (Figure 1). If we examine the other part of the original curve (Figure 10), we get another new curve (Figure 12). We placed again a new trend line, which is fit to the points of Figure 12 (points after 70th peak). Figure 12 shows the equation of the 3rd curve and the determination coefficient, which is 0.9853. This approximation is also a good one.

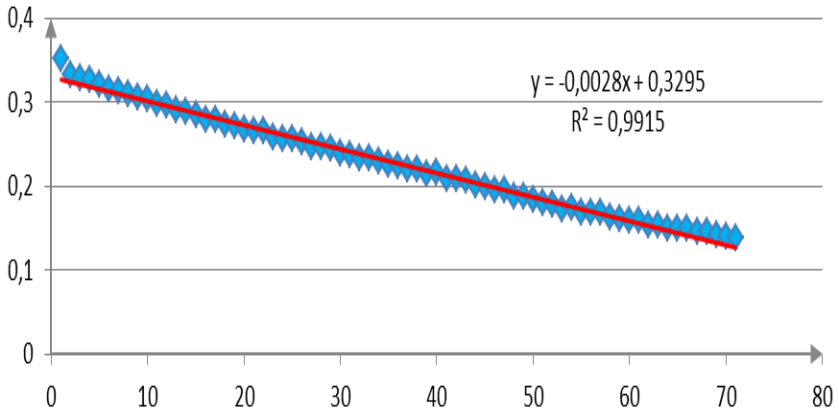

Figure 11. The first part of the curve, the new trend line
(abscissa: number of positive peaks, ordinate: the value of the peak in mm)

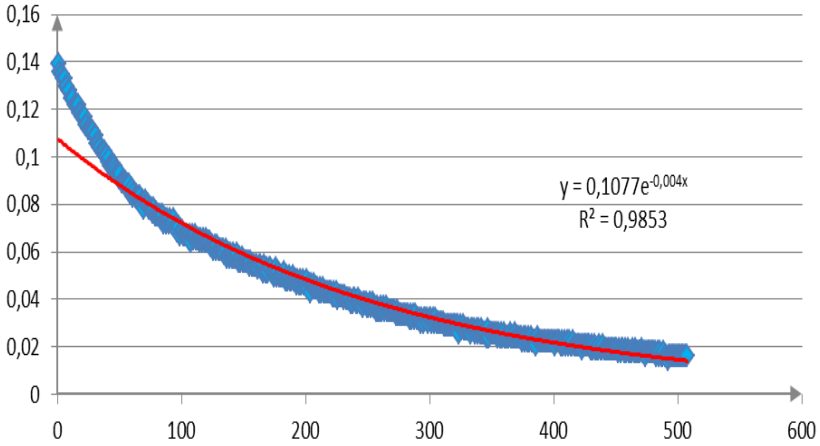

Figure 12. Curve after the 70th peak
(abscissa: number of positive peaks, ordinate: the value of the peak in mm)

4. Evaluation of results

Conclusion from the measured and calculated results is that the vibration damping behaviour of the examined metallic foam until approximately the first 70 peak is Coulomb type damping, after the first 70 peak is a viscous damping type. The behaviour of metallic foam was independent from the loads (1 kg, 2 kg, 3 kg).

5. Acknowledgement

The research work presented in this study based on the results achieved within the TÁMOP-4.2.1.B-10/2/KONV-2010-0001 project and carried out as part of the TÁMOP-4.1.1.C-12/1/KONV-2012-0002 "Cooperation between higher education, research institutes and automotive industry" project in the framework of the New Széchenyi Plan. The realization of this project is supported by the Hungarian Government, by the European Union, and co-financed by the European Social Fund. Admatis Ltd. gave us the metallic foam materials.

6. References

[1] SARKA, F.–DÖBRÖCZÖNI, Á.: Using Metal Foams in gear-drives to reduce the emitted noise. *Design of Machines and Structures*, Vol. 4, No. 1 (2014), 65–75.
[2] ORBULOV, I. N.: *Szintaktikus fémhabok.* PhD-értékezés, 2009.
[3] KORPOSNÉ KELEMEN, K.–KAPTAY, Gy.–BORSIK, Á.: *Fémhabok – A gépter-vezés potenciális szerkezeti anyagai.*
[4] MAKHULT, M.: *Gépágyazások rezgéstani méretezése*. Akadémiai Kiadó, Budapest.

Design of Machines and Structures, Vol. 5, No. 2 (2015) pp. 55–59.

ON DESIGN METHODOLOGY

ÁGNES TAKÁCS
University of Miskolc, H-3515 Miskolc-Egyetemváros, Hungary
takacs.agnes@uni-miskolc.hu

Abstract: It is absolutely not an easy job even for those researchers who are very good at design methodology to find their way in that polemics that rules this field of research. Present paper tries to clear up the difference between the concept and the embodiment, the conceptual design process and the embodiment design.

Keywords: *design methodology, design ability, conceptual design, embodiment design*

1. Introduction

It is hard to explain the difference between concept and embodiment, as in this field of research there are researchers all over the World, so references are written almost all languages of the World. In many cases it is difficult to find the proper word for notions during translating them to our own language. The situation is easier in case of those research fields that have a history of more hundred years and we can order specific figures to certain notions (e.g.: analysis or theoretical research of gears, planetary gears etc.). Design methodology slightly has 60 years behind [1] and as it can be regarded in many ways as design psychology [2], [3] it is rather theoretical science. This leads to different notions should be cleared up once in a while.

2. The whole design process

"Design involves a continuous interplay between what we want to achieve and how we want to achieve it." Suh [10]

The general process of the traditional design is shown in Figure 1, after VDI. The process according to the figure shows maybe the most comprehensively the general picture of the whole design process. Huge disadvantage of the introduced process (and those ones that were determined by the researchers of the classical design methodology) is that it does not make a sharp difference between conceptual and embodiment design. In this figure these two phrases cannot be even found! Significant German authors of classical design methodology – Hansen [4], Rodenacker [8], Koller [6], Roth [9] – regarded working out a method for embodiment design as their primary task, so to help the not-so-experienced designers during their work. As computer era has been started in the 70's their secondary aim was to get their methods to be suitable for a computer algorithm. They did pioneer work in the field so there was no need to find passageways between processes they suggested. Pahl and Beitz [7] defines conceptual design as the part of the whole design process where the designer engineer determines the basic solution routes after the identification and abstraction of the task, defining function-structure, finding and combining the proper solution principles and the elaboration of solution ideas.

Conceptual design and embodiment design have quite different steps. Conceptual design can be characterised by collecting, organising and reorganising ideas with a result of a product idea that is suitable for further embodiment design. During conceptual design neither materials nor sizes are ordered to the concept, this will be important during the embodiment design. The task of the engineering designer during embodiment design is to order the proper sizes, materials and masses to each subassembly and to the whole product embodiment.

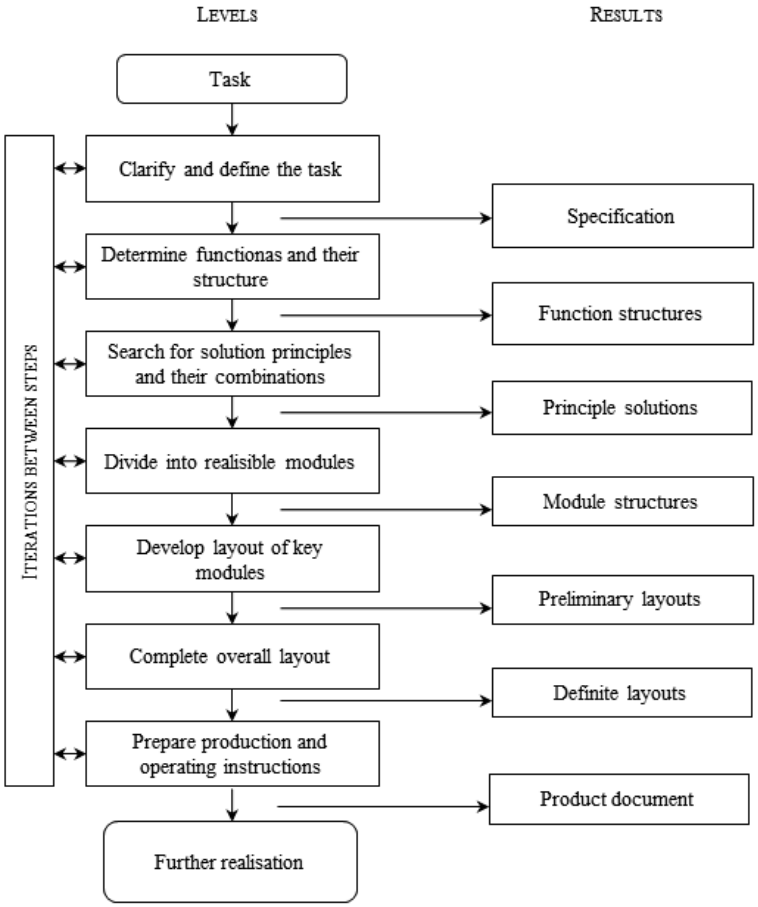

Figure 1. General design process [7], [13]

At the same time Figure 1 very well illustrates that during the whole design process every step has the effect on the other (even earlier, or later). So it should be laid down that without knowing the steps of the whole design process preliminary and getting acquainted with the interference of the steps products, machines, equipment that are optimal solutions of any design issues according to every aspects (economical, environmental, producing, maintenance etc.) cannot be designed.

3. Design process aided by computer

The development of the methodological design was necessary because of the designer who wanted to design the best product in spite of the rushing world and the less time he has got to develop a product. So the significant researchers of this field of science were suggested methods that help the work of the designer-engineer in the phase of conceptual design. Analysing other technologies integrated into CAD systems – so the CAxx technologies – in connection with the whole design process it can be defined that aiding of the design process by computer was developed counter direction to the advancement of it (Figure 2). Computer technologies appear first time in the documentation period of the design process that can be taken as the last phase of it, while the computer aid of conceptual design – that can be taken as the basis of the design – is not yet solved even today! Designers have to keep their eyes on the costumer's criteria as well, although these criteria can eliminate some originally new solutions. This way in this paper a method is suggested that combined with the tool system of the design methodology can be used with a great benefit in the period of conceptual design that is during the working out of the basis of the optimal product variant, and it also pays attention for the costumer's criteria.

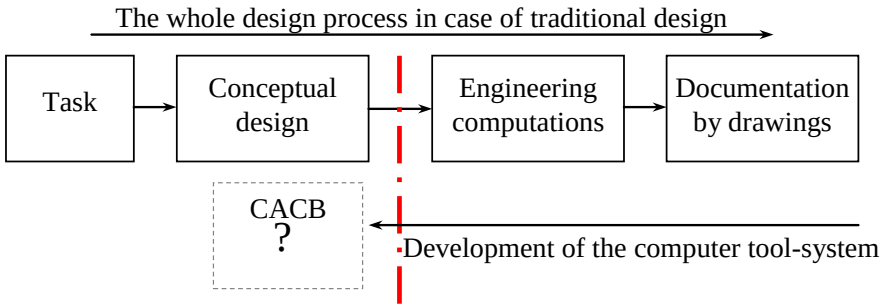

Figure 2. Challenges of the computer adaptation during the application in the design process

4. Conceptual Design process

Logical steps of conceptual design is shown in Figure 3. Before elaborating the design task it should be analysed. The tools for that are the market research and the analysis of patented solutions. In parallel with this customer's requirements should be found and defined. These requirements should be evaluated and ranked with the designer's eyes, because these requirements are the basis of the evaluation at the end of the concept building method. All the possible functional subassemblies should be defined during the market research and the analysis of patented solutions. Product structures or solution variants can be generated from these subassemblies. These variants should be evaluated by the designer. The optimal solution that is the result of the concept building is the one that fulfilled all the evaluation criteria.

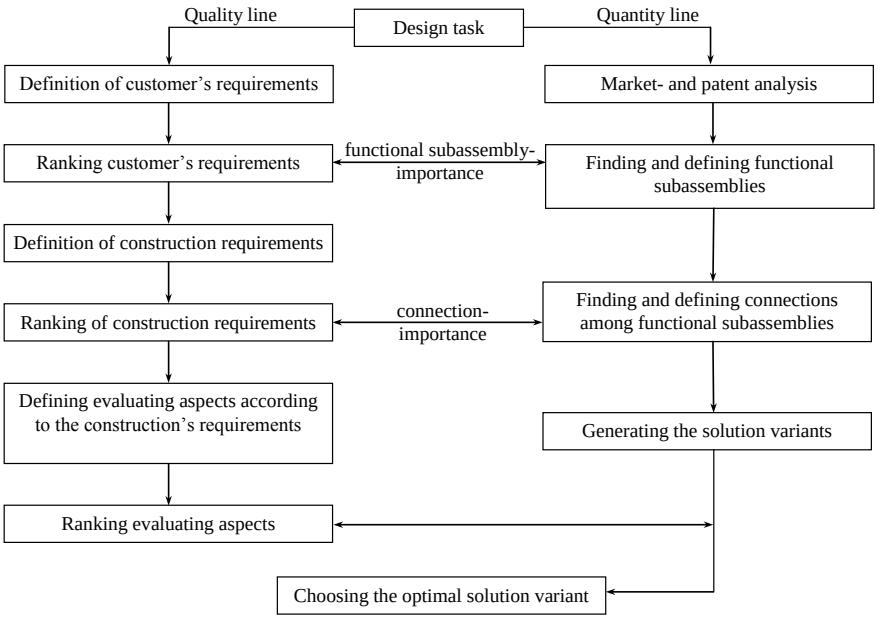

Figure 3. Logical steps of conceptual design suggested for computer [11]

5. Conclusion

Designer engineer prefers development and exploration than generating another example of an existing, similar solution. [5] Reaching this he intends the biggest amount of the time he has for the whole design task for knowing and finding previous solutions. This is the key of the conceptual design, the successful generation of the optimal concept. Nowadays the work of the designer engineer is aided by several, different software but the phase of the conceptual design aided by computer should be still developed. [12]

6. Acknowledgement

The research work presented in this study based on the results achieved within the TÁMOP-4.2.1.B-10/2/KONV-2010-0001 project and supported by the European Union and the State of Hungary, co-financed by the European Social Fund in the framework of TÁMOP-4.2.4.A/2-11/1-2012-0001 'National Excellence Program'.

7. References

[1] BADKE-SCHAUB, P.: Creativity and innovation in industrial design: wishful thinking? *Journal Design Research*, Vol. 5, No. 3, 2007, 353–367.

[2] CROSS, N.: A history of design methodology. In: VRIES, M. J. de et al. (ed.): *Design Methodology and Relationships with Science, NATO ASI Series, Series*

D: Behavioural and Social Sciences. Vol. 71, 1993, Kluver Academic Publishers, Netherlands, 15–27.
[3] CROSS, N.–CLAYBURN CROSS, A.: Expertise in Engineering Design. *Research in Engineering Design,* Springer Verlag, London, 1998, 10, 141–149.
[4] HANSEN, F.: *Konstruktionssystematik; Grundlagen für eine allgemeine Konstruktionslehre.* Verlag Technik, Berlin, 1968.
[5] JONES, J. C.: *Design Methods.* Wiley, Chichester, UK, 1981.
[6] KOLLER, R.: *Konstruktionsmethode für den Maschinen-, Geräte- und Apparatebau.* Springer Verlag, Berlin, 1976.
[7] PAHL, G.–BEITZ, W.–FELDHUSEN, J.–GROTE, K. H.: *Engineering Design – A Systematic Approach.* Third edition. Springer-Verlag, London, 2007.
[8] RODENACKER, W. G.: *Methodisches Konstruieren.* Springer Verlag, Berlin, 1976.
[9] ROTH, K.: *Aufbau und Handhabung von Konstruktionskatalogen.* VDI-Verlag, Düsseldorf, 1974.
[10] SUH, N. P.: *The Principles of Design.* Oxford University Press, Oxford, 1990.
[11] TAKÁCS, Á.: *Számítógéppel segített koncepcionális tervezési módszer*. PhD Thesis, Miskolc, 2010.
[12] TAKÁCS, Á.–KAMONDI, L.: On Design Theories-Fundamentals of a Neuvel Approach. *International Journal of Advanced Engineering,* Vol. 5, No. 1, 2011.
[13] VDI-Richtlinie 2221: *Methodik zum Entwickeln und Konstruieren technischer Systeme und Produkte*. VDI Verlag, Düsseldorf, 1993.

REVIEWING COMMITTEE

Secreteriat of the Vice-Rector for Research and International Relations
University of Miskolc
Responsible for the Publication: Prof. Dr. Tamás Kékesi
Editor: Dr. Ágnes Takács
Published by the Miskolc University Press under leadership of Attila Szendi
Technical editor: Csilla Gramantik
Proofreader: Krisztina Mátrai
Responsible for duplication: Erzsébet Pásztor
Number of copies printed: 50
Put the Press in 2015
Number of permission: TNRT–2015–399–ME
HU ISSN 1785-6892 in print
HU ISSN 2064-7522 online